

Fossil maerl beds as coastal indicators of late Holocene palaeo-environmental evolution in the Bay of Brest (Western France)

Ehrhold Axel ^{1,*}, Jouet Gwenaél ¹, Le Roy Pascal ², Jorry Stephan ¹, Grall Jacques ³, Reixach Théo ⁴, Lambert Clément ⁵, Gregoire Gwendoline ⁶, Goslin Jerome ¹, Roubi Angelique ¹, Penaud Aurélie ², Vidal Muriel ², Siano Raffaele ⁷

¹ IFREMER, Géosciences Marines LGS, Centre de Brest, B.P.70, 29280 Plouzané, France

² Université Européenne de Bretagne Occidentale, UMR-6538 Géosciences Océan, IUEM/CNRS, Place Copernic, 29280 Plouzané, France

³ Université Européenne de Bretagne Occidentale, UMS3113 Observatoire Marin, OSU-IUEM, Place Copernic, 29280 Plouzané, France

⁴ Université de Perpignan, UMR 7194 Histoire naturelle de l'homme préhistorique, Via Domitia 52 avenue Paul Alduy, 66860 Perpignan, France

⁵ Université de Bretagne Sud, UMR 6538 Géosciences Océan, F-56000 Vannes, France

⁶ INTECHMER, LUSAC/CNAM, Boulevard de Collignon, 50110 Turlaville, France

⁷ IFREMER, DYNECO Pelagos, Centre de Brest, B.P.70, 29280 Plouzané, France

* Corresponding author : Axel Ehrhold, email address : axel.ehrhold@ifremer.fr

Gwenael.Jouet@ifremer.fr ; Pascal.Leroy@univ-brest.fr ; stephan.jorry@ifremer.fr ; Jacques.Grall@univ-brest.fr ; theo.reixach@univ-perp.fr ; clement.lambert@univ-ubs.fr ; gwendoline.gregoire@lecnam.net ; Jerome.Goslin@ifremer.fr ; angelique.roubi@ifremer.fr ; Aurelie.Penaud@univ-brest.fr ; muriel.vidal@univ-brest.fr ; Raffaele.Siano@ifremer.fr

Abstract :

The Bay of Brest (BB) is a mixed, tide-dominated estuarine system. The shore terraces of this bay are occupied by modern free-living (calcareous) coralline algae locally termed “maerl”, organized in bed-like morphologies (rhodolith deposits). Cores retrieved from around the bay reveal fossilized primitive maerl beds of Holocene age, interbedded in sandy-silt sedimentation. The alternation between biogenic constructions and estuarine sedimentation may provide evidence of varying environmental conditions of the late-Holocene period. This paper mainly focuses on the results of chronostratigraphic and bio-sedimentological interpretations of coring data collected in less than 15 m of water depth in an attempt to decipher the main stages of maerl colonization in the bay. In particular, this study raises several significant points allowing to draw links between centennial to millennial-scale climatic changes in marine estuary sedimentation and episodes within the development of maerl biocenoses. The paleo-bathymetry of the coastal terraces has not changed significantly over the last 5000 years. Yet, the first maerl occurrence only appeared around 2000 cal yr B.P., likely showing that the environmental conditions were not favorable for their emergence prior to that time. Pioneer maerl beds developed on coarse shell deposits inherited from the paleostorms affecting the Atlantic coasts during the colder climatic period of the Iron Age (3100–1950 cal yr B.P.). The accumulations then aggraded at various and discontinuous rates,

sometimes reaching up to 2.1 m/kyr. Maerl beds temporarily disappeared in the southern part of the Bay of Brest when sedimentation rates increased throughout the bay during the Dark-Age cold period (1375–1250 cal yr B.P.), suggesting that maerl formations could not keep up with sedimentation rate exceeded a certain threshold. Muddy sedimentation conditions also dramatically changed on two occasions, with the establishment of coarse storm levels, set at the intervals 825–600 cal yr B.P. (MWP) and 113–0 cal yr B.P. But maerl deposits reseed the environment as a result of each new cold period, demonstrating the persistence of such coralline algae against drastic palaeoenvironmental changes in coastal areas.

Highlights

► Stratigraphy of late-Holocene estuarine sediments reveals interbedded maerl beds. ► First maerl occurrence in the Bay of Brest is dated around 2000 cal yr BP. ► Development of maerl beds coincides with the onset of colder and drier climates. ► Maerl building phases are disrupted by periods of climate deterioration. ► Coarse sedimentary deposits are associated with increased paleostorm activity.

Keywords : Rhodoliths, Lithothamnion corallioides, stratigraphy, estuarine sedimentation, storm impact, Brittany

1. Introduction

Maerl beds are living and dead aggregations of free-living non-geniculate coralline algae that gather to form extensive beds that may accumulate over time to form fossil deposits. In the Bay of Brest, maerl deposits are formed by free living corallines algae of the *Lithothamniaceae* and *Lithophyllaceae* families. In Europe, different maerl-

forming species are found in shallow waters of the inner shelves from Norway to the north of Portugal and in the Mediterranean Sea to the south (Kamenos et al., 2017). They are found in particular abundance along the coast of Brittany (Grall, 2002) as well as in the Galician rias (Peña and Bárbara, 2009) and Ireland (Bosence, 1976). They occupy the subtidal zone down to ca. 40 m water depth (Hall-Spencer et al., 2010; Teichert et al., 2012) where the abundance of living maerl reaches up to 9000 thalli/m².

Over their long geological history, coralline algae colonized almost all types of marine substrates within the photic zone worldwide as their present-day representatives (Kamenos et al., 2017). They are important ecosystem engineers that produce hard, three-dimensional substrates (Schubert et al., 2020). Calcareous coralline algae are the most common and widely distributed groups of fossilized marine benthic algae since the Late Cretaceous and particularly in the Early Miocene (Aguirre et al., 2000). Fossil coralline algae data are increasingly exploited in palaeoecological studies and reconstruction of palaeoenvironments (Cabioch et al., 1995; Foster, 2001; Burdett et al. 2011; Aguirre et al., 2012; Sarkar, 2017). Recently, Mg/Ca ratios measured in limestone skeletons proved useful for producing environmental reconstructions over the last century (Halfar et al., 2003; Kamenos et al., 2008; Kamenos et al., 2012; Kamenos et al., 2017). Strong relationships have been recorded between Mg/Ca ratios and Sea Surface Temperature (SST) in relation to the North Atlantic Oscillation (NAO) and the Atlantic Multi-decadal Oscillation (AMO) over the past century (Gamboa et al., 2010; Halfar et al., 2007, 2011).

Appropriate conditions for maerl bed development were shown to be generally reached during transgressive periods (Friebe, 1993; Bosence et Wilson, 2003; Nalin et al., 2008; Leszczynski et al., 2012) when the sea-level floods coastal environments. The Highstand Systems Tract (HST) and more particularly the maximum flooding period seems to represent the most favorable palaeoenvironmental conditions for the settlement and expansion of maerl production areas on internal coastal areas if combined with the absence of massive terrestrial inputs (Aguirre et al., 2012). The Glenan Islands in SW Brittany have the thickest known maerl deposit in the world, with accumulations up to 10 m thick reported by Augris and Berthou (1990). Grall and Hall-Spencer (2003) dated a thallus sampled at the subsurface of the deeper part of the excavation area at 5860 cal yr B.P. At the same depth but tens of kilometers to the south-east on the marine terrace of Belle-île Island, the first occurrence of fossil maerl is dated at 5300 cal yr B.P. (Ehrhold et al., unpublished data).

The main aim of this study is to document the stratigraphic and palaeoenvironmental evolution in the Bay of Brest (BB) over the last 2000 cal yr B.P. by using the evolution of fossil maerl beds as a sensitive geological “proxy” of coastal environment fluctuations under climatic and anthropogenic forcings. Maerl beds are of strong ecological importance and conservation value (Grall and Hall-Spencer, 2003). The Bay of Brest was recently the subject of

studies to better constrain the Holocene geological and palaeoenvironmental data (Goslin et al., 2013; Gregoire et al., 2016; 2017; Garcia-Artola et al., 2018; Lambert et al., 2018; 2019; 2020). By integrating new sedimentary records and a new chronostratigraphic framework, the analysis of depositional sequences provides information on the conditions of the development of past maerl beds and the impact of recent climatic events in the context of major landscape changes in the Bay of Brest watersheds.

2. Study area

2.1 Geological and environmental settings

The Bay of Brest is located in northwestern Brittany (NW France, Fig. 1) and constitutes a shallow, semi-enclosed coastal basin of 180 km² surrounded by a 230 km-long rugged coastline. The bay is sheltered from the Iroise Sea and Atlantic storms by an elongated NE-SW narrow strait (the “Goulet”), one nautical mile wide and 50 m deep (Lowest Astronomical Tide or LAT). Many small coves of a few square kilometres such as those of Roscanvel, Fret, Lanveoc-Poulmic, Daoulas and Auberlacher in which the water depth does not exceed 10 m, constitute an essential geomorphological feature of the bay, representing 47% of the marine surface (foreshore included). The peninsula of Plougastel-Daoulas separates the bay into two distinct parts, the estuary of the Elorn river to the north and the estuary of the Aulne river to the south. Beyond 10 m water depth, a set of tidal channel networks inherited from the flow of the Elorn and Aulne rivers during the glacial periods plays an important role in the modern hydrodynamical and sedimentological context in each part of the bay. They converge and connect upstream from the Goulet (Gregoire et al., 2016, 2017; Fig. 1).

The basement of the bay and surrounding rocky coasts are composed of Brioverian rocks structured by an inherited Hercynian fault system. This N70°E trending fault system separates two regional geological domains composed of the peneplanation of the high Hercynian granitic chain to the north (Leon metamorphic domain) (Chauris and Hallégouët, 1980; Ballèvre et al., 2009; Le Gall et al., 2014) and the main fault and sedimentary rocks to the south (Brioverian and Palaeozoic) which form the whole rocky basement of the bay (Babin et al., 1969; Garreau, 1980; Ballèvre et al., 2014). The study area has subsided since the Eocene and is now considered to experience very limited (0.02 to 0.04 mm/yr; Ziegler, 1992; Bonnet et al., 2000) to no subsidence (Poitevin et al., 2019). The palaeo-fluvial network is established since the Cenozoic (Hallégouët et al., 1994). Palaeo-channels of the two main current rivers, Aulne and Elorn, are respectively about 30 and 15 m deep, and converge to the west in a unique valley of about 60 m

deep outside the Goulet (Gregoire et al., 2017). Gregoire et al. (2017) characterized the chrono-stratigraphy of the sediment infilling as corresponding to the late transgressive system track since 10000 cal yr B.P. according to the final stage of deglacial sea-level rise (Camoin et al., 2012). The area switched from a strictly continental domain during late glacial to a ria confined in the main palaeo-fluvial network at early Holocene. Between 10000 and 7000 cal yr B.P., the still rapid sea level rise (up to 10 cm/yr) caused a fast backstepping of the intertidal area recorded by a first transgressive system tract (TST1) and weathered by a tidal incised surface in response to the development of a strong tidal circulation around 7500 cal yr B.P. Between 7000 and 3000 cal yr B.P., the slow retreat of the shoreline coupled with modest accommodation space allowed the development of a second transgressive interval (TST2) characterized by subtidal deposits associated with the migration of tidal bars in the central part of the bay and the growth of tidal flats in the shallowest embayments.

The period of the highstand deposit extends from 3000 cal yr B.P. to the present day. Its lower limit corresponds to the maximum flooding surface (MFS) dated between 3000–2000 cal yr B.P. (Gregoire et al., 2016) when sea-level was almost as high as that of the present day (Goslin et al., 2015). The approximate maximum flooding in such a confined sedimentary system occurred somewhat late compared to the highest sea level imprinted in open-marine bays of the Atlantic (Chaumillon et al., 2010; Tessier et al., 2012) and could be linked to a different organization of the coastal wedges in response to local low sediment supply (Baum and Vail, 1988).

2.2 Palaeoenvironmental conditions and human activity

Climate variability of the Brittany lowland during late Holocene has been well documented (Fernane et al., 2014; Tréguer et al., 2014; Lambert, 2017; Lambert et al., 2018, 2019, 2020; Penaud et al., 2020). The geomorphological (Regnault et al., 1996; Van Vliet-Lanoë et al., 2014a, 2014b, 2016) and sedimentological (Goslin et al., 2013; Stéphan et al., 2015) responses of the Brittany coasts have been examined on decadal to multi-centennial time scales.

During the late Holocene, between 2700 and 2340 yr B.P., the re-activation of dune belts at the tip of the Finistere region reflected a strengthening of storm activity along the French Atlantic coasts (Regnault et al., 1996; Stéphan, 2008; Van Vliet-Lanoë et al., 2014a, 2014b, 2016; Poirier et al., 2017; Pouzet et al., 2018). The base of the channels of coastal streams was observed to have experienced scouring and subsequent exacerbated infilling (Goslin et al., 2013; Stéphan et al., 2015), likely in response to the major increase in precipitations and terrigenous sedimentation observed at European scale.

Between 2400 and 1900 cal yr B.P., Lambert (2017) and Lambert et al. (2020) described the increase in the share of riparian forest and primary production in the BB, simultaneous to the expansion of agropastoralism that began at the end of the Neolithic (4150 yr B.P.) and intensified during the Bronze Age (Marguerie et al., 2001; Gaudin, 2004; David, 2014). This agricultural activity also coincides with the extent of land clearing during the Iron Age (2750-2002 yr B.P.) and the decline of mid-latitude forest cover (Dark, 2006; Meurisse, 2007; Roberts et al., 2018). From 1700 cal yr B.P., the establishment of *Corylus*, a pioneer species in plant recovery, could coincide with a collapse of the local agricultural system (Galliou, 1991; Lambert et al., 2020). Lambert et al. (2020) and Fernane et al. (2014) indicate a revival of forest taxa (more than 30% compared with the previous period) up to 1450 yr B.P. This corresponds to a rapid decrease in agro-pastoral activities in the catchment basins with the combination of oceanic and atmospheric configurations with evidence of increased humidity and storms (Lambert et al., 2020).

Between 1450 and 1100 cal yr B.P., all palynological records collapsed (Lambert, 2017; Lambert et al., 2020). This period coincides with the onset of a colder and drier climate (Dark Ages Cold Period, Wanner et al., 2008; Helama et al., 2017) and the drying-up of sedimentary inputs, notably from 1200 B.P. (RCC5, Mayewski et al., 2004;). Galliou (1991) estimates that it is likely that the collapse of the agricultural system of Roman Armorica caused the desertification of more than 75% of villages in the middle of the 5th century AD, resulting in a decline in cultivated areas and a return of secondary plant formation (Galliou, 1991; Cassard, 1996). This period is marked in most European regions by a stable forest cover or afforestation (Kaplan et al., 2009; Roberts et al., 2018).

From 1100 cal yr B.P., climatic conditions induced arid settings and regular westerly storms over north-western Europe (Van Vliet-Lanoë et al., 2014a, 2014b). Urbanization developed and cereal cultivation increased (Lambert, 2017) while forests regressed, representing only 60% of French territory (Mather et al., 1999). Until the 13th century, forests in France were cut back by nearly 15 million hectares (i.e. 30 to 40,000 hectares/year). This major deforestation was followed by the decrease of *Alnus* around 200 years later and anthropization reached its maximum around 750 yr B.P. dominated by a maximum of *Cerealia* and *Cannabaceae* (Fernane et al., 2014). The retreat of Brittany's forests is in line with that on the European-scale (Williams, 2003; Kaplan et al., 2009). Three centuries of relative stability ensued, corresponding to the Medieval Warm Period MWP (Hughes and Diaz, 1994; Goosse et al., 2006), during which harvests were more abundant, and the European population tripled. Simultaneously, monastic communities developed, particularly in the Aulne catchment area (construction of the abbeys of Landevennec with its new 11th-century Romanesque abbey church, Daoulas in 777 yr B.P., and Relecq in 818 yr B.P.). With the support of the local population, these constructions participated in the region's mass deforestation (Dufief, 1998), along with

massive use of wood in the form of charcoal for mineral processing and as fuel. From the 11th-century onwards, damming on the rivers developed, limiting sediment supply to the coast (Van Vliet-Lanoë et al., 2016).

From 650 years B.P. onwards, plague epidemics (Black Death) drastically reduced populations with more than a third of the European population decimated (Mather et al., 1999). Farms were abandoned and the forests regenerated throughout the territory up to 500 B.P. (Mather et al., 1999). To this episode of decline in human activity corresponded a sharp increase in storminess, responsible for the last major episode of dune formation in Brittany between 600 and 400 cal yr B.P. (Van Vliet-Lanoë et al., 2014a, 2016; Pouzet et al., 2018). The Little Ice Age (LIA) that followed this decline was the most recent and most documented event during which glaciers extended globally (Grove, 2001) and moderately cooler temperatures characterized the Northern Hemisphere from about 500 to 50 B.P. (Mann, 2002; Ilyashuk et al., 2019). Finally, the main episode of forest clearance occurred between the 15th and 17th centuries. With the construction of the Arsenal in Brest (1670), local forests were used for shipbuilding (Le Goff and Meyer, 1971). Since the beginning of the 19th-century, the forest area in France has steadily increased (Cinotti, 1996). The industrial revolution, the substitution of wood for fossil fuels, which became widely available thanks to the increase in transport and trade, and the decline in wooden shipbuilding enhanced to forest restoration. Between 1850 and the middle of the 20th-century, the agronomic model in Brittany was based on the parceling of land into wooded embankments (Lambert et al., 2018). The increase in soil erosion and drainage towards rivers is related to the destruction of linear bocage and hedgerows after 1900 (Auzet, 1987).

2.3 Hydrological, hydrodynamic, and modern sedimentary settings

The Bay of Brest is a macrotidal coastal system characterized by semi-diurnal tidal amplitude ranging from 1.2 to 7.3 m (average of 4 m), leading to the presence of extended intertidal flats during low tides (Troadek and Le Goff, 1997). Marine waters flow into the BB at each new tidal cycle with current speed reaching 1 m/s, mainly oriented W-E. Near to the Pointe des Espagnols (Fig. 1), coastal geometry and submarine morphology generate a Venturi effect with strong tidal current reaching velocities up to 9 m/s during the spring, limiting swell influence. In the remainder of the Bay, marine hydrodynamics seem to be largely dominated by tidal currents ranging from 0.25 to 2 m/s. However, due to local winds, the sea can be rough and affects the superficial water mass (Petton, 2010). Short-length but steep waves can hence reach the shore with high obliquity (Pommepuy et al., 1979), resulting in localized erosion of barrier beaches (Stéphan et al., 2005).

In its easternmost part, the BB receives its main freshwater supplies from the Aulne and Elorn rivers, and the smaller Daoulas River (Fig. 1). The BB watersheds are characterized by 2000 km of waterways and most of their

runoff flows into the bay through the Aulne River (114 km long and 36 m³/s of annual flow; Troadec et al., 1997). The Aulne watershed (1842 km²) is about six times the size of the Elorn catchment area. The Aulne and Elorn river outflows contribute up to 85% of total river discharge into the BB (Delmas and Tréguer, 1983). The salinity of the bay is 34.5‰ and shows no evolutionary trend over the last 20 years (Tréguer et al., 2014).

Sediment inputs by the two main rivers represent only 12000 T/yr of suspended sediment matter for the Aulne (Bassoulet, 1979) and 1000 T/yr for the Elorn (Monbet and Bassoulet, 1989). Ehrhold et al. (2016) estimated that terrestrial inputs account for only 10% of the deposition in the bay today, which implies a substantial contribution of detrital input from the outer sea. Also, local reworking of sediments can occur through fishing activities, storm-swells (Hily et al., 1992) or tide currents that may generate higher concentrations of re-suspended muddy sediment in estuaries (Beudin et al., 2013). Most of the sedimentation takes place in the inner zone of estuaries because tidal energy is stronger than river flow (Dyer, 1997; Moskalski et al., 2018). Klouch et al. (2016a) demonstrated that the south-east of the bay is disconnected from the Elorn estuary, which is the area exporting the highest proportion of particles outside the BB.

2.4 Ecology and distribution of modern free-living maerl

In the BB, live maerl thalli (at least 30% of the present seabed) occupies 40 km² of the bay's shallow waters (Fig. 2) corresponding to muddy terraces (tidal flats) at less than 10 m depth (Grall, 2002; Gregoire et al., 2016) and where sedimentation rates are between 0.5 and 3 mm/year (Fig. 2; Ehrhold et al., 2016). The distribution of maerl beds coincides with areas characterized by an annual mean tidal current velocity of less than 0.26 m/s and wave agitation of less than 0.09 m/s (Dutertre et al., 2015). Both species of free-living thalli, *Phymatholiton calcareum* and *Lithothamnion corallioides*, are found mainly in the region of Brest (Grall, 2002). However, other types of maerl species also exist in the BB: those formed by species of the genus *Lithophyllum* with apparently a more estuarine affinity, particularly for *Lithophyllum fasciculatum* (Peña et al., 2013). Despite slow growth rates that vary according to species and region (about 0.25 to 0.6 mm/yr for *P. calcareum*; Adey and McKibbin, 1970; Grall, 2002; Bosence and Wilson, 2003; Kamenos et al., 2008; Halfar et al., 2011), rhodolith accumulations can reach several metres thick. Bosence and Wilson (2003) compiled information on accumulation rates of maerl beds from different temperate and tropical areas, which does not include the BB. Their results show accumulation rates ranging from 0.08 to 1.4 m/kyr in temperate conditions. Maerl beds constitute three-dimensional multi-centimetric structures with a high volume of sediment matrix (about up to 45 to 50% for *Lithothamnion corallioides* through 5 cm thickness of maerl deposit in the BB). Maerl is an important source of modern-day calcium carbonate production (about 100 to 3000 g/m²/yr) in

temperate marine environments (Bosence, 1980; Potin et al., 1990; Freiwald, 1998; Wehrmann, 1998; Martin et al., 2006). The maerl beds of the Brittany coast were found in areas characterized by annual mean water temperatures varying between 12.2 and 13.6°C (Dutertre et al., 2015). In these conditions, the annual biomass growth rate of calcium carbonate in *Lithothamnion corallioides* is estimated to be 43.8% of the initial calcite mass (Potin et al., 1990).

The development and distribution of maerl accumulations are conditioned by various environmental factors that remain difficult to prioritize (Jacquotte, 1962; Cabioch, 1968; Bosence, 1976; Wilson et al., 2004; Dutertre et al., 2015). Maerl-forming species require clear and relatively shallow water to develop their photosynthetic capacity. The maximum water depth of maerl occurrence, mainly conditioned by light and therefore water turbidity, is 30 m in Galway Bay (De Grave et al., 2000), 25 metres in Scotland (Moore, 2014) and 20 to 25 m in Brittany (Dutertre et al., 2015). The transport capacity of the fruticose rhodoliths depends wave agitation and may only move occasionally due to bioturbation and severe storms (Marrack, 1999; Pardo et al., 2019). Maerl beds can be shaped by the swell to form megaripples, but wave energy can rapidly limit the vitality of the maerl-forming species in contrast with encrusting corallines that can live in such highly hydrodynamic environments. If coastal hydrodynamic conditions are too low, fine sediment particles settle, stifling algal growth (Steller et al., 2007). Conversely, in the case of strong hydrodynamics, the fine sediments are re-suspended, inhibiting photosynthetic activity and coarser particles such as sand or broken shells are transported, burying the thalli under the sediment. Maerl beds are consequently very sensitive to sediment input and sediment mobility. In the estuarine domain, river inflows contribute to turbid load, limiting light penetration and inhibiting the regular growth of maerls (Adey and MacIntyre, 1973; Steller and Foster, 1995; Foster et al., 1997; Wilson et al., 2004). In the BB, the maximum growth rate was recorded in summer (July), while it was close to zero in winter (Potin et al., 1990). Coralline algae are very sensitive to sediment influx (Aguirre et al., 2017). Off the Brazilian coast, rhodoliths form one of the largest known living deposits of coralline algae (Amado-Filho et al., 2012). Vale et al. (2018) showed that the turbid plume of the Amazon River mouth is probably the main driver for rhodolith structure and composition as it determines light penetration, and nutrient and organic matter levels. Deterioration of living rhodoliths occurs after being covered for two weeks by 1 mm of fine sediment (Riul et al. 2008; Villas-Bôas et al., 2014), and even sooner if contains a high concentration of organic matter (Wilson et al. 2004; Hall-Spencer et al. 2006). In the case of *Lithothamnion* sp., death occurs after 41 days of being buried by sediments (Villas-Bôas et al. 2014). The negative influence of terrigenous sedimentation on the development of rhodolith beds has been demonstrated in Pliocene deposits in SE Spain (Aguirre et al., 2012). The species that make up the maerl are sensitive to environmental disturbances such as excessive turbidity and a decrease in light intensity

(extraction, fishing, aquaculture, eutrophication, invasive species, Grall and Hall-Spencer, 2003). Sea temperature also strongly influences the specific composition of European maerl beds (Wilson et al., 2004), probably being the main factor affecting their geographical distribution (Adey, 1973).

3. Core acquisition and methods

3.1 Core sampling

Fifty-two Kullenberg gravity cores (10 cm in diameter, 2-5 m in length) were retrieved from the BB during the SERABEQ3 (2015) and the PALMIRA (2017) surveys, and 45 interface sediment cores (10 cm in diameter, 1 m maximum in length) were sampled during the AL2013 and SERABEQ1-LE32 expeditions (respectively in November 2013 and May 2014). All Kullenberg core acquisitions were made onboard the Genavir-Ifremer R/V *Thalia* and the short interface cores on the INSU RV *Albert Lucas* (Fig. 3). The cores were retrieved between 2 m and 15 m water depth from the lowest low-tide level. SERABEQ core locations were determined using the stratigraphic framework interpreted by Gregoire et al. (2017) on the basis of an extensive set of seismic data. Lithological description and photographs were performed directly after core opening on sliced half-core surfaces. Gregoire et al. (2017) already described the lithology of five main Kullenberg cores (SRQ3-KS02-KS34-KS39-KS41-KS44) and discussed the sedimentary infilling of this bay starting around 9000 cal yr B.P. In this study, we focused on the most superficial sediment deposits (upper seismic unit) and more particularly in the shallowest areas of this bay, corresponding to the last HST composed of muddy sediments interbedded with coralline deposits.

3.2 AMS ^{14}C dating

AMS radiocarbon dating was conducted on several cores from the AL2013, SERABEQ and PALMIRA expeditions (tab. 1) using either CaCO_3 from fresh juvenile marine shells (bivalve mollusks with still articulated valves when possible and gastropods such as *Turritella*), bulk benthic foraminifera or algal thalli in fossil maerl beds. These carbonate samples were picked from the sediment using X-ray imagery and washed from adhering particles to remove any external source of older (reworked) carbon. For each sample, AMS ^{14}C dating was performed using a minimum amount of 1.0 mg of pure carbon. Measurements were conducted at the Poznan Radiocarbon Laboratory (Poland) and at Beta Analytics (UK). Absolute dating was corrected for the mean ^{14}C age difference between the atmosphere and oceanic surface waters by applying a reservoir correction (R) of 325 years (Tisnérat-Laborde et al.,

2010) and a regional deviation (DR) for the BB of 46 years. Absolute ages were calibrated using Calib Rev 7.1 software (Stuiver and Reimer, 1993) from the “Intcal13” calibration curve (Reimer et al., 2013), with a confidence level of 95% for the standard deviation (2 sigma). Despite the fact that the sampling was systematically carried out on the outer coralline thallial surface which may represent the most recent carbonate concretion, radiocarbon dates from corallines present a ^{14}C age offset up to 200 years for the most recent ages, compared to the age model defined on other marine species datings, and so were not considered when younger than 400 cal yr B.P. (Fig. 4).

3.3 Fossil maerl bed characterization

In this study, we used the Geotek XCT system which provided digital linear images similar to half or full section X-ray images of cores obtained by X-ray tomography. X-ray computed tomography (XCT) was used to locate fossil maerl beds accumulated in BB coastal sediments and to determine their geometric signature (Fig. 5). XCT imagery is a non-destructive imaging technique able to provide 3-D data of the internal structure of objects, determined mainly by variations in density and atomic composition (Ketcham and Carlson, 2001; Yang et al., 2010). The X-rays are emitted by a micro-focal source and are then detected by a sensor after passing through the core. The software associated with the device then produces images with a resolution of 100-150 μm in TIFF format. For each core, one to three analysis angles were acquired at 0°, 45° and 90°. To better determine maerl beds before sampling (Fig. 5), original imagery was enhanced from edge detection filters using the open-source image-processing program (GIMP software), and more particularly the Neon filter (Sekanina et al., 2011). Image processing is a helpful tool for detecting layer boundaries as a prerequisite for qualitative and quantitative analysis of sediment cores (Bube et al., 2006). The maerl beds described under XCT were numbered from the oldest to the most recent from the base of the cores (Fig. 5). A 2 cm section in the maerl signature recognized by XCT was sampled, dried and weighed. To avoid breaking the maerl thalli mechanically, the sample was then sieved underwater to separate grain size fractions greater than 2 mm, 250 and 50 μm respectively. The sieve refusals were then dried again and the unbroken maerls (fruticose rhodoliths) were separated under stereomicroscope and weighed, together with the broken maerls (fruticose coralline fragments) and associated coarse bulk shells (Fig. 6). Lastly, the sediment matrix below 250 μm was counted. Two classes of fruticose rhodoliths were considered (Fig. 7): (1) a percentage of dead thalli between 5 and 25% of the total weight for the 2 cm section and (2) a percentage exceeding 25%. For the unsampled maerl beds recognized by XCT signature and the lithological description, a third class was defined considering at least 5% of thalli presence. Fossil maerl fragments were sampled within the identified facies for further identification. Morphological as well as cell

arrangement analyses showed that all fossil maerl fragments sampled belonged to the species *Lithothamnion corallioides*.

4. Results

The succession of mixed siliciclastic-carbonate deposits was examined over the seven coastal zones that cut through the BB from the Roscanvel cove in the west, to the Aulne estuary in the east, and north of Brest commercial harbor at the outlet of the Elorn river. Modern sedimentation is characterized by mixed sediment with a muddy fraction in more or less concentrated (Gregoire et al., 2016). This characteristic is due to estuarine dynamics, influenced by the seabed morphology of the BB and controlled by tidal currents in deep water areas. Based on granulometric analyses and lithological descriptions, three main sedimentary facies have been described in the cores selected for this study. Sandy-silt sediments with a mean percentage of silt and clay of more than 65 % correspond to the original estuarine sedimentation accumulated on tidal flats under low-energy conditions. This facies also constitutes the sediment matrix between the thalli in the maerl beds. Two others classes of sediment are interbedded in the lithology succession and associated with a high energy event: *i*) a thin layer of sand (Ssd for Sand sedimentary deposit), moderately to relatively poorly sorted, composed of medium to coarse sand (more than 70 % of granulometric distribution) mixed with finely crushed bioclasts and, *ii*) a thick layer of coarse shelly debris (Csd for Coarse sedimentary deposit) poorly sorted, for which granulometric classes of sand and gravel constitute more than 60% of the weight of the sample. The last represents the maximum flooding surface at the base of the highstand system tract in the BB (Gregoire et al., 2017). The Holocene shallow marine deposits observed in this study reflect these conditions but also show abrupt stratigraphic changes in the muddy deposit sequence at the scale of the BB. They are denominated as major Coarse Sedimentary Events (CSE) associated with basal erosive surfaces. The age of the base of the fossil maerl beds as well as the main erosive surfaces, at the origin of time gaps were fixed for each area on the basis of local radiocarbon datings (Table 1).

4.1 The Roscanvel cove (RC)

In the inner zone on the seafloor of Roscanvel cove (less than 10 m water depth), the oldest muddy sediments (older than 4000 cal yr B.P.) present, locally, some horizontal laminae rich in plant debris and are associated with *Turritella* shelly levels and other coastal gastropods typical of a sheltered environment. In the outer zone beyond 10 m

depth (towards the open sea), this homogeneous and continuous sandy-silt sedimentation is well observed in core SRQ3-KS39, between 123 and 193 cm below the seafloor (bsf), and after 167 cm (bsf) in core SRQ3-K40, but seems to correspond to older sediments (more than 7000 cal yr B.P.). However, the most recent muddy deposits succession (after 2000 cal yr B.P.) presents some interbedded maerl beds (MB1 to MB5) in the sandy-silt series. The oldest preserved fossil maerl bed or First Maerl Occurrence (FMO-MB1-KS39) is dated between 1850 and 1932 cal yr B.P. and the youngest at about 1365-1418 cal yr B.P. (MB4-KS39). In RC, four high-energy coarse-grain levels of variable thicknesses are also found intercalated between the muddy and carbonate units. The bases of these coarse deposits (CSE) lie on erosional surfaces which lead to variable time gaps. The coarse-shell sediments (CSE1 and CSE2) (Fig. 7a, cores SRQ3-KS39 and KS40) are thicker and probably represent the accumulation of several high-energy episodes that have washed out the fines from the sediment. The erosional events associated with CSE1 (core SRQ3-KS39), dated at around 5135 cal yr B.P. at 123 cm (bsf), have reworked and eroded at least 3000 years of deposits until 7800 cal yr B.P. The event associated with CSE2 (end dated around 1530 cal yr B.P.) often presents a fining-upward sequence, and is followed by the establishment of a first maerl bed (cores SRQ3-KS39 and KS40). The sedimentary layer corresponding to CSE3 (Fig. 7a) becomes thicker at the edge of the terrace (core SRQ3-VZ29). The hydrodynamic event related to these coarse CSE3 deposits is sealed around 577 cal yr B.P. and erodes down to 1245 cal yr B.P. (core SRQ3-KS39). In RC (Fig. 7a), exclusively in the very shallow water zone ($Z < 5$ m), the first coarse-grain level is a well-sorted homogeneous sand associated with the CSE4 event (Fig. 7a, cores SRQ1-IS03 and IS30), with some angular elements at the base. It represents one or more contemporary events centered on 0 B.P. The superficial sediments are characterized by sandy-silt (Fig. 7a) containing the *Crepidula* gastropod and shows low sedimentation rates (1.2 mm/yr. Ethollet et al., 2016). This muddy sedimentation evolves along the northern edge of the coastal terrace towards coarse sand deposits (core SRQ1-IS30) that become thicker with increasing depth (core SRQ3-VZ29).

4.2 The Fret cove (FC)

In the inner zone, between 5 and 10 m water depth (Fig. 7b), below the CSE2 deposit, the sedimentation dated before 3100 cal yr B.P. (core SRQ1-IS04) is homogeneous and contains many large bivalves with their two shells adjoined. In the outer zone, basal sandy-silt deposits at 122 cm and 140 cm (bsf) respectively for cores SRQ3-KS28 and SRQ3-KS27, are similar granulometrically and in age to those found in RC. The event associated with CSE1 began before 4900 cal yr B.P. (Fig. 7b, cores SRQ3-KS38), reworking and eroding at least 3000 years of deposits. The foot of the terrace, beyond 15 m water depth, was subjected to a more active tidal dynamic between CSE1 and CSE2 events.

However, CSE2 is thinner than in RC. Its upper termination with a fining-upward sequence reflects decreasing hydrodynamic settings during this episode of coarse sedimentation. The fine estuarine sedimentation then took place with the development of the first maerl occurrence at around 1873 cal yr B.P. (FMO-MB1-KS38), age is estimated from the age-depth model of RC. This age is concomitant with the one determined in RC. The succession of lithological facies in core SRQ3-KS38 is similar to that found in RC core KS39, located at the same water depth but 3 km further west. At this location, up to 9 levels of maerl beds can be distinguished, with the last-extracted bed (MB9) having an extrapolated age of 1271- 1249 cal yr B.P., with only two levels remaining in the deeper core SRQ3-KS27 ($Z > 15$ m). Unlike in the neighboring bay, the high hydrodynamic conditions persisted after CSE3 and eroded the littoral mud deposits until the extrapolated date of 1170 cal yr B.P. In the internal area, recent sandy-silt sediments rich in fine shell debris lying on the CSE2 coarse sedimentary deposit do not contain maerl beds.

4.3 The Lanveoc-Poulmic cove (LPC)

At the edge of the littoral terrace (cores SRQ3-KS32 and KS35, Figs. 3, 8) maerl beds and sandy-silty sediments constitute the main deposit succession. It is based on a coarser shell level (CSE2) particularly thick on core KS32 (more than 45 cm). The maerl deposits, on the other hand, are more developed, than those described in RC and FC, and include 10 levels of taphocoenoses between CSE2 and CSE3 (MB1 to MB10 in core SRQ3-KS32), although it is not uncommon to encounter a few isolated fruticose coralline fragments in the muddy-silty sediments. Taking into account the absence of more complete data, it is difficult to precisely locate CSE2 and CSE3 in chronological order. Conversely to the two more western coves, the succession of maerl deposits in the LPC occurs at the top of all interface cores taken from the inner area (depth < 10 m). The proportions of fruticose rhodoliths can reach more than 70% in some layers (with an average ranging from 30 to 50%, Fig. 8). The development of these biocenoses, common to all infralittoral samples (cores SRQ1-IS23-IS24-IS25-IS26-IS28) below 7 m water depth, is interrupted by a decimetric and homogeneous fine-grain broken shell sand deposit associated with the CSE4 erosive surface. The regional hydrodynamic event causing the deposition of this sandy level and the erosion of the underlying sediment is dated to the 1940s, considering the sedimentation rates (0.05 cm/yr, Fig. 2) recorded in this part of the BB (Ehrhold et al., 2016). In the more eastern part of the bay, a pluri-centimetre layer of coarser and poorly-sorted broken shells was deposited around 50 cm (bsf) (cores IS23 and IS24), probably resulting from a change in local hydrodynamic conditions along the Lanveennec coast.

4.4 The Aulne estuary (AE)

With the exception of core SRQ1-IS16 (Fig. 9), which has characteristics close to those of its neighboring cores in LPC with four successive maerl deposits (MB1 to MB4), the grain size of the upper sedimentary layers of the other cores reflects the intensity of the currents triggered by the channeling of the Aulne River (Fig. 1). Hydrodynamics is responsible for the reworking and mixing of highly eroded coarse-grain shelly sediments that are poorly sorted, and sometimes finer on shallower flats (core SRQ1-IS13). Hypothesizing for a constant sedimentation rate between 2020 cal yr B.P. (92 cm bsf) and 1492 cal yr B.P. (35 cm bsf), the first maerl occurrences are estimated to have appeared around 1950 cal yr B.P. (FMO-MB1-KS20). After the establishment of these first maerl communities, only a few taphocoenoses are preserved, either due to turbidity conditions in the estuarine zone, which were probably not very favorable for the development of coralline algae, or to erosion processes.

4.5 The Daoulas cove (DC)

In the open southern zone (Fig. 3), beyond 2 m water depth, fossilized maerl beds are older (up to 500 cal yr B.P.) for MB1-SRQ1-IS21. The very shallow zone (water depth $0 < 2$ m) presents the same succession of sedimentary deposits and maerl beds as in LPC (Figs. 8, 10) south of the Aulne Channel, with fossil maerl beds (four to five successive accumulations; MB1 to MB5) interbedded with sandy-silt layers. Based on a constant sedimentation rate between 15 and 66 cm (bsf) in core SRQ1-IS07, these maerl beds probably developed recently and since approximately 234 cal yr B.P. Core SRQ1-IS20 is distinguished by a coarse-sediment layer composed of fruticose coralline fragments, at 15 cm (bsf), and of a mixture of crushed shells. These layers are probably inherited from the action of fishing dredges on the seafloor at an earlier time, as the extraction of maerl by dredging started only at the beginning of the 20th-century. The proportions of biogenic coarse mixture in the surface layer (more than 40%) reflects the action of dredges of the clam *Venus verrucosa* fishery (Ragueneau et al., 2018; Bernard et al., 2019). Only the most confined sectors of the bay, to the west (core SRQ1-IS11) and to the north (core SRQ1-IS09), show respectively bioturbated and laminated sediments with a high sedimentation rate (4 mm/yr in Klouch et al., 2016b) that hinders the development of maerl beds.

4.6 The Auberlac'h cove (AC)

In cores KS34 and KS36 the stratigraphic organization is identical to those described within the same water depth ranges in the other sectors of the bay (Roscanvel, Fret and Lanveoc-Poulmic coves). However, the distribution of maerl deposits is denser, with up to 11 preserved maerl beds to the top of the CSE2 episode (SRQ3-KS34 core) estimated at 1914 cal yr B.P. The first preserved maerl deposit (SRQ3-KS34-MB1) overlies the roof of CSE2 at the

origin of the deposition of coarse shelly sediments and the erosion of the underlying sediments. It is therefore dated to 1914 cal yr B.P. based on sedimentation rates extrapolated from the age model (Figs. 11-12). The percentages of maerl in place in the fossil beds show that they are not the densest (5 to 26%) in the whole area, probably due to the location of this core located in the Aulne paleo-channel that guides flux of suspended matter (Gregoire et al., 2017). Sedimentation rates increase very rapidly by a factor of two from 2000 cal yr B.P. (1.02 mm/yr) until the 1400-1300 cal yr B.P. (2.07 mm/yr) interval, then decrease sharply after this maximum (1.57 mm/yr around 1000 cal yr B.P.) and collapse after the CSE3 episode (0.41 mm/yr) (Fig. 12). For comparison, modern sedimentation rates in the BB are of the order of 0.45 mm/yr (Ehrhold et al., 2016), i.e. five times less than during the Merovingian era (1474-1199 B.P.). In the inner zone (water depth $Z < 6$ m), as in the LPC, the sedimentary succession is characterized by a multi-centimetre sandy, finely shelly level located 5 cm (bsf), with a base corresponding to the CSE4 event (Fig. 11). In the external zone, the CSE4 event has not been recorded and the maerl accumulations are less numerous (two to three) until the CSE3 episode which ends around 700 cal yr B.P. (Fig. 12). Below, four levels of maerl beds are interspersed at least up to 410 cal yr B.P. age (MB1 to MB5 in core AL2013-1508).

4.7 Brest harbor and the Elorn estuary (BEE)

This is the region of the bay that presents the most complex organization and succession of sedimentary facies (Fig. 13), probably linked to the development of Brest's commercial port since the Second World War and the lateral migration of the Elorn channel in time and space. The sedimentary evolution is therefore even more controlled here than in the other sectors of the bay by the hydrodynamic processes due to river action, Atlantic storm swell penetration and strengthened local winds. The first maerl occurrence is dated to around 1940 cal yr B.P. (SRQ3-KS04-MB1), concomitant with the end of the coarse deposit associated with CSE2. This taphocoenose is preserved on the core PALM-KS05 (216 cm bsf), and was probably almost reached at the base of core SRQ3-KS04. In core SRQ3-VZ33, the resumption of fine sedimentation occurs later than in other regions of the bay (1332 cal yr B.P. at 66 cm bsf), simply because the location of this core is more directly related to the strong tidal dynamic of the channel, as previously shown by Gregoire et al. (2017), who described coarse deposits associated with erosive processes. The erosive base of the CSE3 deposit evolves locally between 1008 cal yr B.P. (core SRQ1-IS32) and 829 cal yr B.P. (core PALM-KS03 in Delebeq et al., 2020) estimated from the local age-depth model (4 mm/yr between 22.5 and 45.5 cm (bsf)). The core PALM-KS05 sampled from the artificial sector of the commercial port (Fig. 3) shows a time gap above the CSE3 deposits (Fig. 13) which would have removed about 1 m of sandy-silt deposit and maerl levels, taking into account the 2.35 mm/yr average sedimentation rate calculated over this period. In the internal zone (water depth $Z <$

10 m) on the northern (core PALM-KS05) and southern (core SRQ3-KS04) flats on both sides of the channel, the well-conserved sedimentary archives show respectively the intercalation of up to 15 and 11 maerl beds between the FMO and the CSE3 event. On the overall area, the surface layer consists of a mixture of coarse and sandy elements with some fruticose coralline fragments (cores SRQ1-IS17-IS19 in the north and IS03 in the south). The fraction of fruticose rhodoliths never exceeds 4%. In shallow water depths, the sandy deposit associated with the CSE4 event is not present.

5. Discussion

The partitioning of the Bay of Brest, due to its very indented coastline, the inherited submarine topography that strongly guides estuarine and tidal dynamics, and the presence of two estuaries attached to distinct catchment areas implies that the factors controlling the overall sedimentation (i.e. hydrodynamism, climate, sea-level, and anthropism) and the maerl deposits must be examined using all results obtained for at least 3000 years B.P. for the overall study area (Fig. 14). Based on our observations, the successive occurrence of maerl beds and of major regional sedimentary events can be divided into three main phases.

5.1 The CSE2 sedimentary crisis of the Iron Age and the appearance of first maerl occurrence during the Gallo-Roman period

Despite a large and well-distributed number of stratigraphic samples (97 cores), we did not find any levels of fossil maerl beds older than 1950 cal yr B.P. in the sedimentary records of the BB (Fig. 14). Considering a relative mean sea-level of 1 m below modern sea-level at 2000 yr B.P. (García-Artola et al., 2018), the maximum depth at this date corresponding to the first maerl occurrence is 15-16 m in front the FC (MB1-SRQ3-KS27-KS38, Fig. 7b) and of the LPC (MB1-SRQ3-KS32, Fig. 8). This implies considering a water depth limit identical to that of maerl beds in front of the Pointe de Pen Ar Vir (Fig. 2). It can be also noted that between 1910 and 1970 cal yr B.P., the seeding of muddy sediments by these pioneer maerl thalli was common along all coastal terraces of the BB. The dominant species was composed of more than 90% of *Lithothamnion corallioides*, as is the case today (Grall, 2002). *Phymatoliton calcareum* and notably the species with webbed strands *Lithophylum fasciculatum* were much rarer. This period of first occurrence is very close to the 1842 ± 320 cal yr B.P. age obtained by Wehrmann (1998) on a maerl level sampled at 160 cm (bsf) and at 15 m water depth near the Bay of Morlaix (northern coast of Brittany; Fig. 1).

A major question surrounds the absence of maerl beds older than 2000 cal yr B.P., at least for 5000 years corresponding to the end of the CSE1 episode. Indeed, several regional records of relative sea-level (Stéphan, 2008; Goslin, 2015; García-Artola et al., 2018) indicate that the relative local sea-level at the early Bronze Age was around -5 m below present sea-level, i.e. just below the level of present-day lowest low tides. Correspondingly, the morphological terraces (T3 in Gregoire et al., 2017) suitable for autochthonous accumulations of maerl-forming species were already partly submerged. Even considering the effect of the tidal range (± 5 m), the physiognomy of the seafloor at water depths less than 15 m and the light irradiance necessary for photosynthesis of coralline plants were likely already similar to modern environmental conditions. Maerl beds could have developed to a water depth of 15 m as they did after 2000 yr B.P., and still today in the vicinity of the Pointe de Pen Ar Vir (Fig. 2).

Several studies have shown that thick rhodolith deposits imply long time spans (Bosence et Wilson, 2003), and are preferentially established during setting of transgressive contexts (Malin et al., 2008; Leszczynski et al., 2012) and highstand systems tracts (Aguirre et al., 2012), under conditions of terrigenous starvation and moderate hydrodynamics (Aguirre et al., 2017). Gregoire et al. (2017) and Stéphan (2008) showed a rapid stratigraphic backstepping of the BB coastline from 5500 to 3000-2000 cal yr B.P., accompanied by the establishment of mature salt marshes and a first generation of gravel and pebble barriers. Sedimentary archives along the coasts of Brittany and notably those to the south (Glenan archipelago, Fig. 1) record that massive maerl accumulations appeared as soon as 5862 ± 57 cal yr B.P. (Grall & Spencer, 2003). The maximum flooding surface, which represents the point of maximum shoreline transgression when the Holocene relative sea level rise slowed down (Tessier et al., 2012), was reached in the BB around 3000 cal yr B.P. and persisted until 2000 cal yr B.P. (Gregoire et al., 2017). This implies that a rather low sediment input allowed maximum retrograding of the bay line to have occurred before the transition to tidal hydrodynamics and the emplacement of prograding deposits (Baum and Vail, 1988, Tessier et al., 2012). Despite this conjunction of favorable conditions from at least 3000 cal yr B.P. (and likely even from around 5000 cal yr B.P.), no trace of fossil maerl of this age is found in the BB sedimentary records, suggesting that, either some environmental factors did not allow the establishment and preservation of maerl beds, or, to a lesser extent the latter were not preserved due to the erosive potential of CSE1 and CSE2.

The first maerl occurrences (Fig. 14) were established in the BB above a succession of coarse multi-decimetre thick shell deposits (CSE2_B, Fig. 12) marked at its base by an erosive surface. The thickness of these coarse deposits records the intensity of the reworking undergone by the underlying sandy-silt sediment they rest on. This sedimentary episode is recorded across the BB, except in the very shallow depths ($Z < 5$ m) with the exception of the commercial port. Between 5 and 10 m water depths, the thickness of the coarse deposits is decimetric, and pluri-decimetric beds

occurred below 10 m water depth. At shallow water depths ($Z < 5$ m), the erosive events and associated time gaps are not very well recorded. On the slope break of the coastal terrace (between 6-15 m depth), erosion may be consequent and merge with the similar but older CSE1 episode (5500-6000 cal yr B.P.), even reaching the coarse-grained deposits interpreted as the glacial lag deposit (LST, Gregoire et al., 2017) and the bedrock for cores SRQ3-KS35-KS36 on either side of the Aulne paleo-channel. The hydrodynamic event(s) at the origin of this Csd sequence can be dated between 3100 and 1950 cal yr B.P. This morphogenic episode ends earlier in front of the Aulne estuary (2100 cal yr B.P.). This time lag is probably an expression of the geographical situation of the mouth of the Aulne estuary, which is more protected from the agitation by the waves. Several ^{14}C dates have been made across this coarse deposit, and yielded ages quite evenly spread between 3000 and 2000 cal yr B.P. (3005, 2836, 2250, 2192, 2025, cal yr B.P.). Although due to the reworking nature of this deposit, they can only be integrated except for provide a temporal framework for the processes responsible for this interruption in fine sedimentation. The normal graded bedding at the end of the succession provides information on the progressive decrease in energy in the environment.

This coarse interbedded deposit common to all the sedimentary sequences described in the BB evokes similar coarse-grained layers (coarse grain sedimentation pulse CGP), described on the Atlantic coasts (Regnauld et al., 1996; Stéphan, 2008; Poirier et al., 2017; Pouzet et al., 2018) and northern Europe (Van Geel et al., 1996; Sorrel et al., 2012) all dating back to 3300 to 2000 cal yr B.P., i.e. during the Iron Age period at the Subboreal–Subatlantic transition (Fig. 15d-h). This could be assimilated to a condensed toplap deposit described by Kondo et al. (1998) in the upper unit of HSTs representing events of storm sedimentation in exposed shallow-marine fossiliferous deposits on the Sea of Japan coast. This interval is associated with significant climatic cooling of North Atlantic surface waters and continental temperatures in Western Europe (RCC4 between 2500-3500 B.P. in Mayewski et al., 2004), likely controlled by a 1450-year-old North Atlantic climate cycle (Poirier et al., 2017). Van Vliet-Lanoë et al. (2014a) recorded significant morphogenic episodes at 2350 and 2060 yr B.P. in the dune belts of the Bay of Audierne to the south of the BB (Fig. 1 and Fig. 15f). Even the southwestern sector of the BB, which is sheltered from stormy waves, was affected by the energy of the sea and winds that can occur during successive winters and are sufficient to remobilize biogenic debris down to 15 m water depth. This sediment reworking is concentrated under the effect of tidal currents, leading to an exacerbated flattening of estuaries and erosion of dune barriers (Stéphan, 2008; Goslin, 2014; Van Vliet-Lanoë et al., 2014a, 2016). Pouzet et al. (2018) describe the same high energy facies at 100 cm bsf near Anno Domini within very sheltered marsh deposits of the protected north-northwestern coast of the island of Yeu (Fig. 15d).

5.2 The maerl expansion phase up to CSE3 sedimentary events during the Medieval Warm Period (MWP)

The maerl deposits developed in the BB (all sub-regions combined, Fig. 14b1-b2-b3) almost continuously during the 1970-840 cal yr B.P. period. Even though the seabeds of the southeastern part of the BB with the LPB, AE, DB and AB are the best represented in terms of analyzed data, the three sub-regions of the bay (Fig. 14b1-b2-b3) present a similar disturbance at 1375 cal yr B.P. up to 1250 cal yr B.P. This interruption in the almost continuous evolution of the fossil maerl beds at the regional scale reflects a major environmental change with enhancement of discontinuous development of maerl accumulations until 840 cal yr B.P., corresponding to the beginning of a new major sedimentary episode (CSE3). For the sediment cores in which the alternation of maerl beds and sandy-silt levels is well dated (tab. 2, SRQ3-KS34 and SRQ1-IS28), mean accumulation rates of maerl beds in the BB derived from local sedimentation rate curves (Figs. 12 and 16), are within the range of the measurements compiled by Bosence and Wilson (2003) for temperate waters, and even slightly higher, with rates varying from 1 m/kyr to 2.1 m/kyr. However, these results show that the construction periods of the maerl beds are not linked systematically to a reduction in sedimentary flows and the resulting deposition of suspended particles. Sedimentation rates do not necessarily fall during periods of maerl accumulation (for example considering a reduction of 50%), and this would be reflected by a drift in the age model (Fig. 16). So it is challenging to define the evolution of sedimentation rate at the time of the maerl beds formation. It is also likely that for the same period, the sedimentation of estuarine suspended sediment matter above maerl beds was slightly lower than that of the local sedimentation rate outside the maerl bed. Green et al. (1998) and Beudin et al. (2013) showed that dense concentrations of benthic mollusks on the seabed as in the case of *Crepidula* gastropods or horse mussel bivalves, increase seabed roughness parameters and the frictional forces above the dense assemblages, and reduce sedimentation processes and could even initiate resuspension. This may be one of the factors responsible for the development of maerl beds under current estuarine sedimentation conditions ranging from 0.5-3 mm/yr in the BB (Dutertre et al., 2015; Ehrhold et al., 2016), whilst the annual growth rate of this coralline algae is very slow (about 0.25 mm/year in BB, Potin et al., 1990; Grall, 2002). Consequently, below a certain maximum threshold of sedimentation (about 2.5 mm/yr) and turbidity in the water, other environmental factors are probably responsible for the rapid variations in fossil maerl deposits over time. However the thickness of the maerl beds and their formation time seems to react to the evolution of the sedimentary environment with a common rule whatever the period considered (Fig. 17). The definitive thickness of the fossilized maerl bed is the result of the agglomeration of maerl thalli. The ratio between the ages of the maerl beds calculated on the basis of age-depth model compared to the theoretical ages normalized by the average annual growth (tab. 2) shows that the thickness of the maerl deposits increases twice as fast during periods of high sedimentation rates. This may be a physiological

response of the maerl bed to maintain a level of vitality in response to the stress imposed by excess sedimentation in the BB, somehow similar to the keep-up strategies adopted by coral reefs in response to relative sea level rise. For other organisms, such as corals, high-turbidity conditions on reefs do not always impact negatively on their physiology (Perry, 2005; Anthony, 2006). Anthony and Fabricius (2000) found that corallite growth rates in *Porites* species nearly doubled under turbidity loads.

In the historical post-RWP (Roman Warm Period) period of the first maerl occurrence, a multi-decadal succession of maerl accumulations is observed in our sedimentary records, but cannot be explained by the first results we obtained. Understanding the origin of this high-frequency variability will require to resort to new, higher-resolution approaches, by tightening the age models and using other environmental proxies. Several physical-chemical factors play a role in the growth and reproduction of coralline algae such as the variation in the calcium concentration in seawater (Martin et al, 2006), the nitrate concentration (Martin et al, 2007), macroalgal epiphyte abundance (Quinmet et al., 2018) or temperature variations (Dutertre et al, 2015). All these factors can be modulated by the combined influences of atmospheric and oceanic configurations and the pressure of man on the environment over very short periods of time.

Our study shows that maerl beds in the Bay of Brest flourished after the high-intensity marine weather episodes of the Iron Age and an increase in the share of riparian forest (Lambert, 2017; Lambert et al., 2020). This period gave way to an improvement of climatic conditions during the climatic optimum of the Upper Roman Empire (between 2060 and 1900 cal yr B.P.), favorable to human colonization of coastal sites (Meurisse, 2007) and to agro-pastoralism. At the end of this period, during which a short, colder and a drier climate persisted (Fernane et al., 2014; Fig. 15j) and lead to reduced terrigenous sediment influx into the Bay of Brest, (Fig. 12) the development of maerl beds affected the entire seabed of the region. Two centuries of prolonged drought reduced agricultural productivity in the catchments (Galliou, 1991) and restored tree vegetation (Fernane et al., 2014; Lambert, 2017; Fig. 15c), probably beneficial to maerl biocenoses. However, sedimentation rates gradually increased from 1800 cal yr B.P. and then accelerated in the BB from 1600 cal yr B.P. to reach a maximum between 1450 and 1250 cal yr B.P (Figs. 12, 16). Since 1800 cal yr B.P. this rate then doubled in the southern part of bay over a few centuries, and almost tripled in the northern BB, with values five times higher locally than those measured today in front of the AC (Ehrhold et al., 2016). This gradual increase in sedimentation rate of the bay, coincides with the increase in terrigenous inputs observed on other environmental proxies (Fig. 15c), particularly palynological (*Corylus*) by Lambert et al. (2020) and with the synchronous disappearance of maerl beds around 1375 cal yr B.P. throughout the southern BB. It can be assumed that the amounts of suspended solids and associated deposition exceeded the capacity of biocenoses to remain in place

during this short period. This signal of terrigenous input was observed by Durand et al. (2018) in the estuary of the Loire (Fig. 15a), and Lambert et al. (2020) based on arboreal taxa pollen characterization (increase in *Corylus*, Fig. 15c). Pears et al. (2020) note that from 1600 to 1400 yr B.P., the accumulation rates increased in the Severn River (south-west UK), with evidence of large flood events associated with the climatic deterioration of the Dark Age Cold Period (Fig. 15m). From 1250 cal yr B.P. when a new, colder and drier climate period occurred (Fig. 15l), combined with the drying-up of sedimentary input (RCC5, Mayewski et al., 2004), maerl biocenoses developed again. In most regions of Europe, this period is marked by moister conditions (Fig. 15k-l), stable forest cover (Fig. 15b) or small forest recovery (Kaplan et al., 2009; Corella et al., 2013; Helama et al., 2017).

From about 850 cal yr B.P., the bio-sedimentary record of the BB seafloor, in areas deeper than 15 m water-depth, is truncated by a new erosive event that left a decimetric deposit of sediments that were more sandy than a shell-bed (Ssd, CSE3 in Fig. 12). Even if dating is missing to better specify the end of the event(s) at the origin of this temporal *hiatus*, we suppose that it would have ended around 600 cal yr B.P. as observed at Roscanvel and Auberlacher coves (Fig. 7). Nevertheless, two datings performed on material sampled within this interval allow to situate the erosive event responsible for this deposit between 834 and 614 cal yr B.P. The erosive impact is more pronounced in Fret and Roscanvel coves than anywhere else on the bay's coast (erosion respectively up to 1245 to 1167 cal yr B.P.). The related sandy deposit is not found in the shallow waters of the south-eastern area of the BB due to a lack of long cores. This sand deposition in the Elorn estuary erodes the underlying sediment at least until 825 cal yr B.P. Differential erosion as a function of geography and the nature of the seafloor can be an indicator of the preferential wind direction that drives sediment remobilization processes, with a strengthening of northerly winds and consequently an increase in fetch distance and in the height of wind-waves towards the south shore of the bay. This period of enhanced paleo-storminess was also found to be responsible for the disturbance of Yeu's environment at the beginning of the LIA (Pouzet et al., 2018, Fig. 15d). Van Vliet-Lanoë et al. (2014b, 2016) and Poirier et al. (2017) show that the MWP was originally responsible for considerably modifying the coastal morphology of Brittany under the action of regular stormy winds. A succession of eleven major paleostorms was recorded in the Brittany dune belts (Fig. 15f) between the 10th and 12th centuries (Van Vliet-Lanoë et al., 2016). At the same time and from 1100 cal yr B.P., Brittany forests retreated (Fig. 15c), as did European forests (Fig. 15b) (Mather et al., 1999; Williams, 2003; Kaplan et al., 2009) in conjunction with the development of monastic communities in the region, contributing to a profound modification of watersheds (Dufief, 1998). It seems that the sedimentation conditions in the BB controlled by anthropic and climatic effects throughout the MWP and until the beginning of the LIA, were not conducive to the development of maerl deposits.

5.3 The maerl of modern times

From 600 cal yr B.P. and onwards, the evolution of maerl in the sediment is only continuous until today in the south-eastern region of the BB east of the Auberlac'h-Lanveoc limit (Fig. 14b3). This is also probably the case in the northern parts of the bay, but the extent of maerl beds is limited to the outlet of the Elorn estuary. In the Roscanvel and Fret coves (Fig. 14b1), as in the commercial harbor of Brest (Fig. 14b2), other factors are responsible for its temporary or more permanent disappearance. Consistent with the first major post-RWP maerl occurrence period, maerl deposits re-established in the BB during a new cold event (RCC6, Fig. 15 k-l, in Mayewski et al., 2004): The climatological event of the Little Ice Age typically associated with negative NAO modes, solar lows, and usually reduced precipitation (Van Vliet-Lanoë et al., 2016). In the BB, sedimentation rates collapse during this period and are between three to five times lower than those of the period preceding stage 1000-1100 cal yr B.P. (Fig. 12). The maerl deposit is interrupted by sandy deposition (CSE4 event) which intersperses a temporal *hiatus* of lower intensity and is more localized than in previous climatic events (CSE2 and CSE3). This multi-centimetre deposit is difficult to identify because it is very close to the top of the cores. Moreover, it is not found everywhere in the BB and is limited to very shallow depths (less than 7 m). This sandy level is associated with a limited erosive effect on the silty sediments and the underlying maerl beds. On the south coast in the Roscanvel and Auberlac'h coves, where it is best expressed, it is present since 1830s. The origin of this late and so temporary event is poorly constrained in the BB. Several major well-recorded winter storms impacted the Brittany coasts after the 1800s (Van Vliet-Lanoë et al., 2014b), notably the storm in 74 cal yr B.P. (Tabeaud et al., 2009). It is difficult to know which event would be responsible for this sedimentary remobilization and contribution. The sedimentary record of this episode in the shallow waters between RC and FC may suggest a preponderant action of northerly winds (from northwest to northeast), occurring dominantly during the spring. In the area of Brest's commercial port, this sand deposit is absent from the cores for depths of less than 2m. At depths of up to 7 m, it does not appear clearly, because it is confused with the recent sedimentary dynamics of the Elorn estuary (SRQ1-IS19). Major works were involved in this area during the development and expansion of the commercial port in the 1970s and 1980s. This invisible truncation surface on the lithology of core PALM-KS05 had been described by Delebecq et al. (2020) and on other nearby cores for the study of ancient dinoflagellate communities over time.

The early 20th century should have marked the end of favorable sedimentary conditions for maerl biocenoses with the acceleration of global warming and storm intensity as in previous episodes (3100-1950 cal yr B.P.; 825-600 cal yr B.P.). It is probably too early to say, but several factors may be responsible for slowing down the degradation of

sedimentary conditions (increased turbidity and sediment reworking) in the bay. The lack of terrigenous input from watersheds (Ehrhold et al, 2016) is partly the result of the development of watercourses, particularly the Aulne River with the construction of the Nantes to Brest canal between 1805 and 1842 (Cucarull, 1991). Other factors have indeed limited soil leaching and drainage of watercourses: *i*) the implementation of reforestation and forest management policy throughout Brittany (Gautier, 1938), and *ii*) the break-up of agricultural lands from 1850 to 1950 into many small cultivated plots delimited by slopes and hedges composed of bushes and shrubs (Lambert et al., 2018). However, the changes in maerl occurrence since the Roman period raises questions about the fate of this community in the BB and in a context of rapid climate change (warming waters, heavy rainfall) the introduction of new species to this region (Lejart and Hily, 2011) or the decline of others (Travers et al, 2009). The most recent period, after the Second World War, shows a trend towards a progressive increase in storms on the Atlantic coasts with significant impact on coastal erosion (Wasa, 1998; Drevet, 2002; Lozano et al., 2004; Charles et al., 2012). This period also corresponds to the implementation of a new agricultural policy which led to the reunification of agricultural holdings (Flatrès, 1963). Runoff from the watersheds of the BB is currently increasing, contributing to changes in the trophic conditions of marine waters (Lambert et al., 2018; Ragueneau et al., 2018). Finally, the current maerl biocenoses are locally replaced by a coarse deposit composed of friable coralline fragments and shell debris, as shown on several cores in front of Auberlac'h and Daoulas bays, and in the commercial port, under the action of clam fishing dredges. The muddy sediments reworking upwards through the use of fishing gear will also eventually weaken the habitat of maerl increasing ecological stress due to turbidity (Bernard et al., 2019).

6. Conclusions

Our results allowed to characterize the evolution of maerl beds interbedded in coastal fine sediments deposits over the last 3000 cal yr B.P. in the Bay of Brest (western Brittany NW France). This study highlights the fact that maerl beds record the main evolution of coastal systems in a context of rapid climate change and anthropogenic pressure.

- The fossil maerl deposits (mainly *Lithothamnion corallioides*) develop from 1950 cal yr B.P. above the all muddy marine terraces and down to 15 m water depth, from the northern part of the BB to the southern region with a short time shift. The autochthonous and discontinuous accumulations of maerl beds in coastal areas could have developed above this terrace once the sea reached the highest levels during the late Holocene. Three main periods of maerl bed development have been recorded in the last Highstand System Track: between 1950 and 1350 cal yr B.P.,

between 1250 and 850 cal yr B.P., and since 600 cal yr B.P. These periods coincide with the establishment of cold-climate periods in Europe (RCC in Mayewski et al., 2004) typically associated with negative NAO modes and low solar activity. The cold-climate periods combined with favorable marine morphological factors (shallowest flat terraces, moderate currents) enable maerl aggregations to prosper in the BB environment. The rates of maerl bed accumulation varied from 1 m/kyr to 2.1 m/kyr and seem positively correlated with sedimentation rates.

- Several main periods of climate deterioration have prevented or profoundly disrupted the development of these maerl beds over the last 2000 years. They are associated with increased paleo-storm activity. Their intensity has reworked all the seafloors of the BB and has resulted in the deposition of high-energy sedimentary layers with varying thickness depending on the exposure of the bottom to swells and currents. The CSE2 episode recorded in the form of a poorly sorted and broken shell bed occurred during the 3100-1950 cal yr B.P. period (Iron Age) and coincided in the BB with the MFS (Gregoire et al., 2017). Erosion of underlying sand/silt sediments can be significant in places. Despite its geographical situation, relatively sheltered by the Gorée Strait, the seabed of the BB recorded equivalent morphogenic responses to the increase in storminess to the ones found elsewhere in various environments along the Atlantic and Northern European coasts. The CSE3 episode, dated to 825 to 600 cal yr B.P. (during MWP), was responsible for the deposition of thick sandy layers and the remobilization of coastal marine terraces of the BB down to a depth of 15 m. Sediment erosion associated with major storms is more significant in front of the RC and FC sites, likely indicating a more northerly orientation of the wind sectors during this period. The CSE4 deposits are more limited in time and space. This event or series of events occurred between 113 and 0 cal yr B.P. and mainly affected the very shallow areas (< 7m) of the southern region of the BB.

Acknowledgments

The sedimentological data were collected during the surveys jointly conducted by the French Research Institute for Exploitation of the Sea (IFREMER) and the European Institute for Marine Studies (IUEM, University of Brest) with the collaboration and help of INSU (Institut National des Sciences de l'Univers). The authors are grateful to the officers and crews members of the R/V Thalia (Genavir) and R/V Albert Lucas (INSU) as well as Claire Bossenec for her help during laboratory analysis. Research funds were provided by the Brittany Region as part of the Paleoecology of *Alexandrium minutum* dans la Rade de Brest–Marché n°2017-90292 project PALMIRA, which supported the core sampling, analyses, and post-doc fellowship of ML. This work was made possible thanks to the support of the Laboratoire d'Excellence LabexMer (ANR-10-LABX-19-01) and a grant from the French government under the

program “Investissements d'Avenir”. Main issues of this project are integrated within the theme ‘Dynamics of Human Settlement and Paleoenvironments’ of the Zone Atelier Brest Iroise (ZABrI, INEE-CNRS). We thank Alison Chalm for improvement of the English version. Finally, the authors are very grateful to the two anonymous reviewers for their careful examination of previous versions of this paper and for their helpful comments.

References

- Adey, W.H., 1973. Temperature control of reproduction and productivity in a subarctic coralline alga. *Phycologia* 12, 111-118.
- Adey, W.H., McKibbin, D.L., 1970. Studies on the maerl species *Phymatolithon calcareum* (Pallas) nov. comb. and *Lithothamnium corallioides* Crouan in the Ria de Vigo. *Botanica Marina* 13 (2), 100-106.
- Aguirre, J., Riding, R., Braga, J.C., 2000. Diversity of coralline red algae: origination and extinction patterns from the Early Cretaceous to the Pleistocene. *Paleobiology* 26 (4), 651-657.
- Aguirre, J., Braga, J.C., Martín, J.M., Betzler, C., 2012. Paleoenvironmental and stratigraphic significance of Pliocene rhodolith beds and coralline algal biocostructions from the Carboneras Basin (SE Spain). *Geodiversitas* 34 (1), 115-136.
- Aguirre, J., Braga, J.C., Bassi, D., 2017. Rhodoliths and rhodolith beds in the rock record, in: Riosmena-Rodríguez, R., Nelson, W., Aguirre, J. (Eds.), *Rhodolith maerl Beds: A Global Perspective*. Coastal Research Library 15, Berlin, Springer, Cham, pp. 105-135.
- Amado-Filho, G.M., Pereira-Filho, G.H., Echia, R.G., Abrantes, D.P., Veras, P.C., Matheus, Z., 2012. Occurrence and distribution of rhodolith beds on the Fernando de Noronha Archipelago of Brazil. *Aquat. Bot.* 101, 41-45.
- Anthony, K.R.N., 2006. Enhanced energy status of corals on coastal, high-turbidity reefs. *Mar. Ecol. Prog. Ser.* 319, 111-116.
- Anthony, K.R.N., Fabricius K.E., 2000. Shifting roles of heterotrophy and autotrophy in coral energetics under varying turbidity. *J. Exp. Mar. Biol. Ecol.* 252 (2), 221-253.
- Augris, C., Berthou, P., 1990. Les gisements de maerl en Bretagne. Ifremer report.
- Auzet, V., 1987. L'érosion des sols cultivés en France sous l'action du ruissellement. *Annales de géographie* 537, 529-556.
- Babin, C., Didier, J., Moign, A., Plusquellec, Y., 1969. Goulet et rade de Brest: essai de géologie sous-marine. *Revue de géologie dynamique et de géographie physique UPMC*, 1969, 2° série, XI (1), 55-63.

- Ballèvre, M., Bosse, V., Ducassou, C., Pitra, P., 2009. Palaeozoic history of the Armorican Massif: Models for the tectonic evolution of the suture zones. *C. R. Geosci.* 341 (2-3), 174-201.
- Ballèvre, M., Catalán, J. R. M., López-Carmona, A., Pitra, P., Abati, J., Fernández, R.D., Ducassou, C., Arenas, R., Bosse, V., Castiñeiras, P., Fernández-Suárez, J., Gómez Barreiro, J., Paquette, J.L., Peucat, J.J., Poujol, M., Ruffet, G., Sánchez Martínez, S., 2014. Correlation of the nappe stack in the Ibero-Armorican arc across the Bay of Biscay: a joint French-Spanish project. *Geological Society, London, Special Publications* 405 (1), 77-113.
- Bassoulet, P., 1979. Etude de la dynamique des sédiments en suspension dans l'estuaire de l'Aulne (rade de Brest). University of Bretagne Occidentale, Brest, France (PhD thesis).
- Baum G.R., Vail, P.R., 1988. Sequence stratigraphy concepts applied to Tertiary units, Gulf and Atlantic Tertiary basins, in: Wilgus, C.K., Hastings, B.S., St.C.Kendall, C.G., Posamentier, H.W., Ross, C.A., Van Wagoner J.C. (Eds), *Sea Level Changes: An Integrated Approach*. Soc. Econ. Paleontol. Mineral., Spec. Publ 42, 124-154.
- Bernard, G., Romero-Ramirez, A., Tauran, A., Pantalos, M., Dorlandre, B., Grall, J., Grémare, A., 2019. Declining maerl vitality and habitat complexity across a dredging gradient: Insights from in situ sediment profile imagery (SPI). *Sci. Rep.* 9 (1), 1-12. <https://doi.org/10.1038/s41598-019-52586-8>.
- Beudin, A., Chapalain, G., Guillou, N., 2013. Suspended sediment modelling in the bay of Brest impacted by the slipper limpet *crepidula fornicata*. *Coastal Dynamics* 2013, 193-202.
- Bonnet, S., Guillocheau, F., Brun, J.P., Van Den Driessche, J., 2000. Large-scale relief development related to Quaternary tectonic uplift of a Proterozoic-Paleozoic basement: The Armorican Massif, NW France. *J. Geophys. Res. Solid Earth* 105 (F8), 19273-19288.
- Bosence, D.W.J., 1976. Ecological studies on two unattached coralline algae from western Ireland. *Palaeontology* 19 (2), 365-395.
- Bosence, D.W.J., 1980. Sedimentary facies, production rates and facies models for recent coralline algal gravels, Co. Galway, Ireland. *Geological Journal* 15 (2), 91-111.
- Bosence, D.W.J., Wilson J., 2003. Maerl growth, carbonate production rates and accumulation rates in the northeast Atlantic. *Aquat. Conserv.* 13 (S1), S21-S31.
- Bube, K., Klenke, T., Feudel, U., 2006. An algorithm for detecting layer boundaries in sediments. *Nonlinear. Process. Geophys.* 13 (6), 661-669.
- Burdett, H.L., Kamenos, N.A., Law, A., 2011. Using coralline algae to understand historic marine cloud cover. *Palaeogeogr. Palaeoclimatol. Palaeoecol.* 302, 65-70.

- Cabioch, J., 1968. Quelques particularités anatomiques du *Lithophyllum fasciculatum* (Lamarck) Foslie. *Bulletin de la Société botanique de France* 115 (3-4), 173-186.
- Cabioch, G.M., Montaggioni, L.F., Faure, G., Ribaud-Leurenti, A., 1999. Reef coral-algal assemblages as recorders of paleobathymetry and sea-level changes in the Indo-Pacific province. *Quat. Sci. Rev.* 18, 1681-1695.
- Camoin, G.F., Sear, C., Deschamps, P., Webster, J.M., Abbey, E., Braga, J.C., Iryu, Y., Durand, N., Bard, E., Hamelin, B., Yokoyama, Y., Thomas, A.L., Henderson, G.M., Dussouillez, P., 2012. Reef response to sea level and environmental changes during the last deglaciation: Integrated Ocean Drilling Program Expedition 310, Tahiti Sea-level. *Geology* 40 (7), 643-646.
- Cassard, J.C., 1996. Sur le passé romain des anciens Bretons. *Kreiz (Etudes sur la Bretagne et les Pays celtiques)* 5, 1-33.
- Chaumillon, E., Tessier, B., Reynaud, J.Y., 2010. Stratigraphic records and variability of incised valleys and estuaries along French coasts. *Bulletin de la Société géologique de France* 131 (2), 75-85.
- Chauris, L., Hallégouët, B., 1980. Carte géol. France (1/50 000), feuille de Brest (274) (partie pays de Léon). Orléans: BRGM. Notice explicative sous la coordination de Chauris et Plusquellec.
- Cinotti, B., 1996. Évolution des surfaces boisées en France: proposition de reconstitution depuis le début du XIX^e siècle, *Revue forestière française* XLVIII (6), 547-562.
- Charles, E., Idier, D., Delecluse, P., Déqué, M., Le Cozannet, G., 2012. Climate change impact on waves in the Bay of Biscay, France. *Ocean. Dyn.* 62 (6), 831-848.
- Corella, J. P., Stefanova, V., El Anjoumi, A., Rico, E., Giral, S., Moreno, A., Plata-Montero, A., Valero-Garcés, B.L., 2013. A 2500-year multi-proxy reconstruction of climate change and human activities in northern Spain: the Lake Arreo record. *Palaeogeogr. Palaeoclimatol. Palaeoecol.* 386, 555-568.
- Cucarull, J., 1991. La difficile naissance des canaux bretons, contribution à La Bretagne des savants et des ingénieurs 1750-1825. Rennes, édition Ouest-France 1991, pp. 222-239.
- Dark, P., 2006. Climate deterioration and land-use change in the first millennium BC: perspectives from the British palynological record, *J. Archaeol. Sci.* 33 (10), 1381-1395.
- David, R., 2014. Modélisation de la végétation holocène du Nord-Ouest de la France: reconstruction de la chronologie et de l'évolution du couvert végétal du Bassin parisien et du Massif armoricain. University of Rennes 1, Rennes, France (PhD thesis).

- De Grave, S., Fazakerley, H., Kelly, L., Guiry, M. D., Ryan, M., Walshe, J., 2000. A Study of Selected Maërl Beds in Irish Waters and their Potential for Sustainable Extraction. Marine Resources Series, 10. Marine Institute, Dublin.
- Delebecq G., Schmidt S., Ehrhold A., Latimier M., Siano R., 2020. Revival of ancient marine dinoflagellates using molecular biostimulation. *J. Phycol* 56 (4), 1077-1089. <https://doi.org/10.1111/jpy.13010>.
- Delmas, R., Treguer, P., 1983. Evolution saisonnière des nutriments dans un écosystème eutrophe d'Europe occidentale (la rade de Brest). *Interactions marines et terrestres. Oceanol. Acta* 6 (64), 345-356.
- Drevet, C., 2002. Évolution du nombre de tempêtes observées en France. *La Météorologie* 37, 46-56.
- Dufief, A., 1998. Les cisterciens en Bretagne: XIIe-XIIIe siècles, in : *Annales de Bretagne et des pays de l'Ouest* 105 (3), 131-133.
- Durand, M., Mojtahid, M., Maillet, G., Baltzer, A., Schmidt, S., Blet, S., Marchès, E., Howa H., 2018. Late Holocene record from a Loire River incised paleovalley (French inner continental shelf): Insights into regional and global forcing factors. *Palaeogeogr. Palaeoclimatol., Palaeoecol.* 511, 12-28.
- Dutertre, M., Grall, J., Ehrhold, A., Hamon, D., 2015. Environmental factors affecting maerl bed structure in Brittany (France). *Eur. J. Phycol.* 50 (4), 371-383.
- Dyer, K.R., 1997. *Estuaries: A Physical Introduction*, 2nd edition, Chichester, United Kingdom: Wiley.
- Ehrhold, A., Gregoire, G., Schmidt, S., Jouet, C., Le Roy P., 2016. Present-day sedimentation rates and evolution since the last maximum flooding marine event in the Bay of Brest (W-N France). AGU Fall Meeting, San Francisco (2016), 2016AGUFMEP11A0974E.
- Fernane, A., Gandouin, E., Penard, A., Van Vliet-Lanoë, B., Goslin, J., Vidal, M., Delacourt, C., 2014. Coastal palaeoenvironmental record of the last 7 kyr B.P. in NW France: Submillennial climatic and anthropic Holocene signals. *Holocene* 24 (12), 1785-1797.
- Flatrès, P., 1963. La deuxième « Révolution agricole » en Finistère, in : *Études rurales* 8, pp. 5-55.
- Foster, M.S., 2001. Rhodoliths: between rocks and soft places. *J. Phycol.* 37 (5), 659-667.
- Foster, M.S., Riosmena-Rodriguez, R., Steller, D.S., Woelkerling, W.J., 1997. Living rhodolith beds in the Gulf of California and their implications for palaeoenvironmental interpretation, in: Johnson, M.E., Ledesma-Vázquez, J. (Eds.), *Pliocene carbonates and related facies flanking the Gulf of California, Baja California*. Geol Soc Am Special paper 318, pp. 127-139.
- Freiwal, A., 1998. Modern nearshore cold-temperate calcareous sediment in the Troms District, northern Norway. *J. Sediment Res.* 68 (5), 763-776.

- Friebe, J.G., 1993. Sequence stratigraphy in a mixed carbonate-siliciclastic depositional system (middle Miocene, Styrian Basin, Austria). *Geol. Rundsch.* 82 (2), 281-294.
- Galliou, P. 1991. La Bretagne romaine: de l'Armorique à la Bretagne. Jean-Paul Gisserot ed.
- Gamboa, G., Halfar, J., Hetzinger, S., Adey, W., Zack, T., Kunz, B., Jacob, D.E., 2010. Mg/Ca ratios in coralline algae record northwest Atlantic temperature variations and North Atlantic Oscillation relationships. *J. Geophys. Res.* 115, C12044.
- Garcia-Artola, A., Stephan, P., Cearreta, A., Kopp, R.E., Khan, N.S., Horton, B.P., 2018. Holocene sea level database from the Atlantic coast of Europe. *Quat. Sci. Rev.* 196, 177-192.
- Garreau, J., 1980. Structure et relief de la région de Brest. *Norv. 108* (1), 541-548.
- Gaudin, L. 2004. Transformations spatio-temporelles de la végétation du nord ouest de la France depuis la fin de la dernière glaciation. Reconstitutions paléo-paysagères. University of Rennes 1, Rennes, France (PhD thesis).
- Gautier, M., 1938. La forêt de Loudéac et ses abords depuis le milieu du XVII^e siècle, in : *Presse Universitaire de Rennes, Annales de Bretagne et des pays de l'Ouest* 45 (1-2), pp.72-88.
- Goosse, H., Arzel, O., Luterbacher, J., Mann, M.E., Renssen, L., Riedwyl, N., Timmermann, A., Xoplaki, E., Wanner, H., 2006. The origin of the European "Medieval" Warm Period". *Climate of the Past, European Geosciences Union (EGU)*, 2006 2 (2), 99-113.
- Goslin, J., 2014. Reconstitution de l'évolution du niveau marin relatif holocène dans le Finistère (Bretagne, France): dynamiques régionales, réponses locales. *Géomorphologie*. University of Bretagne Occidentale, Brest, France (PhD thesis).
- Goslin, J., Van Vliet-Lanoë, B., Stephan, P., Delacourt, C., Fernane, A., Gandouin, E., Hénaff, A., Penaud, A., Suanez S., 2013. Holocene relative sea level changes in western Brittany (France) between 7600 and 4000 cal B.P.: Reconstitution from basal-peat deposits. *Géomorphologie: relief, processus, environnement* 19 (4), 425-444.
- Goslin, J., Van Vliet-Lanoë, B., Spada, G., Bradley, S., Tarasov, L., Neill, S., Suanez, S., 2015. A new Holocene relative sea level curve for western Brittany (France): Insights on isostatic dynamics along the Atlantic coasts of north-western Europe. *Quat. Sci. Rev.* 129, 341-365.
- Grall, J., 2002. Biodiversité spécifique et fonctionnelle du maerl: réponses à la variabilité de l'environnement côtier. University of Bretagne Occidentale, Brest, France (PhD thesis).
- Grall, J., Hall-Spencer, J.M., 2003. Problems facing maerl conservation in Brittany. *Aquat. Conserv.* 13, 55-64.
- Green, M.O., Hewitt, J.E., Thrush, S.F., 1998. Seabed drag coefficient over natural beds of horse mussels (*Atrina zelandica*). *J. Mar. Res.* 56 (3), 613-637.

- Gregoire, G., Ehrhold, A., Le Roy, P., Jouet G., Garlan, T., 2016. Modern morpho-sedimentological patterns in a tide-dominated estuary system: the Bay of Brest (west Brittany, France). *J. Maps* 12 (5), 1152-1159.
- Gregoire, G., Le Roy, P., Ehrhold, A., Jouet, G., Garlan, T., 2017. Control factors of Holocene sedimentary infilling in a semi-closed tidal estuarine-like system: the bay of Brest (France). *Mar. Geol.* 385, 84-100.
- Grove, J.M., 2001. The initiation of the “Little Ice Age” in regions round the North Atlantic. *Clim. Change* 48 (1), 53-82.
- Halfar, J., Steneck, R., Schöne, B., Moore, G.W.K., Joachimski, M., Kronz, A., Fietzke, J., Estes, J., 2007. Coralline alga reveals first marine record of subarctic North Pacific climate change. *Geophys. Res. Lett.* 34 (7), L07702.
- Halfar, J., Steneck, R.S., Joachimski, M., Kronz, A., Wanamaker Jr., A.D., 2008. Coralline red algae as high-resolution climate recorders. *Geology* 36 (6), 463-466.
- Halfar, J., Hetzinger, S., Adey, W., Zack, T., Gamboa, G., Kunz, B., Williams, B., Jacob, D.E., 2011. Coralline algal growth-increment widths archive North Atlantic climate variability. *Palaeogeogr. Palaeoclimat. Palaeoecol.* 302 (1-2), 71-80.
- Hall-Spencer, J.M., White, N., Gillespie, G., Gillham, K., Peggo, A., 2006. Impact of fish farms on maerl beds in strongly tidal areas. *Mar. Ecol. Prog. Ser.* 326, 1-6.
- Hall-Spencer, J.M., Kelly, J., Maggs, C.A., 2010. Assessment of maerl beds in the OSPAR area and the development of a monitoring program. Department of Environment, Heritage and Local Government, Ireland, 1-34.
- Hallégouët, B., Lozac'h, G., Vigouroux, F., 1994. Formation de la rade de Brest. Corlaix, J.P. (Eds.), *Atlas permanent de la mer et du littoral*. N°1. University of Nantes. CNRS-URA-904/Editmar, France.
- Helama, S., Meriläinen, J., Tuomenvirta, H., 2009. Multicentennial megadrought in northern Europe coincided with a global El Niño–Southern Oscillation drought pattern during the Medieval Climate Anomaly. *Geology* 37 (2), 175-178.
- Helama, S., Jones, P.D., Briffa, K.R., 2017. Dark Ages Cold Period: a literature review and directions for future research. *Holocene* 27 (10), 1600–1606.
- Hily, C., Potin, P., Floc'h, J.Y., 1992. Structure of subtidal algal assemblages on soft-bottom sediments: fauna/flora interactions and role of disturbances in the Bay of Brest, France. *Mar. Ecol. Prog. Ser.* 85 (1/2), 115-130.
- Hughes, M.K., Diaz, H.F., 1994. Was there a ‘Medieval Warm Period’? *Clim. Change*, 26 (2-3), 109-142.
- Ilyashuk, E.A., Heiri, O., Ilyashuk, B.P., Koinig, K.A., Psenner, R., 2019. The Little Ice Age signature in a 700-year high-resolution chironomid record of summer temperatures in the Central Eastern Alps. *Clim. Dynam.* 52 (11), 6953-6967.

- Jacquotte, R., 1962. Etude des fonds de maerl de Méditerranée. *Rec. Trav. St. Mar. Endoume* 26 (41), 141-235.
- Kamenos, N.A., Cusack, M., Moore, P.G., 2008. Coralline algae are global palaeothermometers with bi-weekly resolution. *Geochim. Cosmochim. Acta* 72 (3), 771-779.
- Kamenos, N.A., Hoey, T., Nienow, P., Fallick, A.E., Claverie, T., 2012. Reconstructing Greenland Ice sheet runoff using coralline algae. *Geology* 40 (12), 1095-1098.
- Kamenos, N.A., Burdett, H.L., Darrenougue, N., 2017. Coralline Algae as Recorders of Past Climatic and Environmental Conditions, in: Riosmena-Rodríguez, R., Nelson, W., Aguirre, J. (Eds.), *Rhodolith/maerl Beds: A Global Perspective*. Coastal Research Library 15, Springer, Cham, pp. 27-53.
- Kaplan, J.O., Krumhardt, K.M., Zimmerman N., 2009. The prehistoric and preindustrial deforestation of Europe. *Quat. Sci. Rev.* 28 (27-28), 3016-3034.
- Ketcham, R.A., Carlson, W.D., 2001. Acquisition, optimization and interpretation of X-ray computed tomographic imagery: applications to the geosciences. *Comput. Geosci.* 27 (4), 381-400.
- Klouch, Z.K., Caradec, F., Plus, M., Hernandez-Fariñas, T., Pineau-Guilleau, L., Chapelle, A., Schmidt, S., Quéré, J., Guillou, L., Siano, R., 2016a. Heterogeneous distribution in sediments and dispersal in waters of *Alexandrium minutum* in a semi-enclosed coastal ecosystem. *Harmful Algae* 60, 81-91.
- Klouch, Z.K., Schmidt, S., Andrieux-Loyer, F., Le Gac M., Hervio-Heath, D., Qui-Minet, Z.N., Quere, J., Bigeard, E., Guillou, L., Siano, R., 2016b. Historical records from dated sediment cores reveal the multidecadal dynamic of the toxic dinoflagellate *Alexandrium minutum* in the Bay of Brest (France). *FEMS Microbiol. Ecol.* 92 (7), fiw101.
- Kondo, Y., Abbott, S.T., Kitamura, A., Kamp, P.J.J., Naish, T.R., Kamataki, T., Saul, G.S., 1998. The relationship between shellbed type and sequence architecture: examples from Japan and New Zealand. *Sediment. Geol.* 122 (1-4), 109-127.
- Lambert, C., 2017. Signature paléoenvironnementale des séquences holocènes en Rade de Brest: forçages climatiques et anthropiques. University of Bretagne Occidentale, Brest, France (PhD thesis).
- Lambert, C., Penaud, A., Vidal, M., Klouch, K., Gregoire, G., Ehrhold A., Eynaud, F., Schmidt, S., Ragueneau, O., Siano, R., 2018. Human-induced river runoff overlapping natural climate variability over the last 150 years: Palynological evidence (Bay of Brest, NW France). *Glob. Planet. Change* 160, 109-122.
- Lambert, C., Vidal, M., Penaud, A., Le Roy, P., Goubert, E., Pailler, Y., Stephan, P., Ehrhold, A., 2019. Palaeoenvironmental reconstructions during the Meso- to Neolithic transition (9.2-5.3 cal ka B.P.) in Northwestern France: Palynological evidences. *Holocene* 29 (3), 380-402.

- Lambert, C., Penaud, A., Vidal, M., Gandini, C., Labeyrie, L., Chauvaud, L., Ehrhold, A., 2020. Striking forest revival at the end of the Roman Period in north-western Europe. *Sci. Rep.* 10 (21984), 1-8.
- Le Gall, B., Authemayou, C., Ehrhold, A., Paquette, J.L., Bussien, D., Chazot, G., Aouizerat, A., Pastol, Y., 2014. LiDAR offshore structural mapping and U/Pb zircon/monazite dating of Variscan strain in the Leon metamorphic domain, NW Brittany. *Tectonophysics* 630, 236-250.
- Le Goff, T.J.A, Meyer, J., 1971. Les constructions navales en France pendant la seconde moitié du XVIII^e siècle. *Annales, Histoire, Sciences Sociales* 26 (1), 173-185.
- Lejart, M., Hily, C., 2011. Differential response of benthic macrofauna to the formation of novel oyster reefs (*Crassostrea gigas*, Thunberg) on soft and rocky substrate in the intertidal of the Bay of Brest, France. *J. Sea Res.* 65 (1), 84-93.
- Leszczyński, S., Kołodziej, B., Bassi, D., Malata, E., Gasiński, M.A., 2012. Depositional history of mixed siliciclastic-carbonate flysch deposits: Paleocene-Eocene transition, Silesian Nappe, Polish Outer Carpathians. *Facies* 58 (3), 367-387.
- Lozano, I., Devoy, R.J.N., May, W., Andersen, U., 2004. Storminess and vulnerability along the Atlantic coastlines of Europe: analysis of storm records and of a greenhouse gases induced climate scenario. *Mar. Geol.* 210 (1-4), 205-225.
- Mann, M.E., 2002. The Little Ice Age, in: MacCracken, M.C., Perry, J.S. (Eds.), *Encyclopedia of global environmental change, volume 1, the earth system: physical and chemical dimensions of global environmental change*. Wiley & Sons Ltd, Chichester, pp. 504-509.
- Marguerie, D., Thenail, C., Lecœur, D., 2001. Armorican bocages and societies: origins, evolution and interactions, in: Barr, C., Petit, S. (Eds.), *Hedgerows of the world*. UK-IALE and CEH, Birmingham, pp. 102-111.
- Mather, A.S., Fairbairn, J., Needle, C.L., 1999. The course and drivers of the forest transition: The case of France. *J. Rural. Stud.* 15 (1), 65-90.
- Martin, S., Castets, M.D., Clavier, J., 2006. Primary production, respiration and calcification of the temperate free-living coralline alga *Lithothamnion corallioides*. *Aquat. Bot.* 85 (2), 121-128.
- Martin, S., Clavier, J., Chauvaud, L., Thouzeau, G., 2007. Community metabolism in temperate maerl beds. Nutrient fluxes. *Mar. Ecol. Prog. Ser.* 335, 31-41.
- Mayewski, P.A., Rohling, E.E., Stager, J.C., Karlén, W., Maasch, K.A., Meeker, L.D., Meyerson, E.A., Gasse, F., van Kreveld, S., Holmgren, K., Lee-Thorpe, J., Rosqvist, G., Rack, F., Staubwasser, M., Schneider, R.R., Steig, E.J., 2004. Holocene climate variability. *Quat. Res.* 62 (3), 243-255.

- Meurisse, M., 2007. Enregistrement haute résolution des massifs dunaires Manche, mer du Nord et Atlantique: Le rôle des tempêtes. University of Lille 1, Lille, France (PhD thesis).
- Moore, C.G. 2014. The distribution of maerl and other coarse sediment proposed protected features within the South Arran pMPA - a data review to inform management options. Scottish Natural Heritage Commissioned Report, 749.
- Moskalski, S.; Floc'h, F.; Verney, R.; Fromant, G.; Le Dantec, N., and Deschamps, A., 2018. Sedimentary dynamics and decadal-scale changes in the macrotidal Aulne River estuary, Brittany, France. *J. Coast. Res.* 34 (6), 1398-1417.
- Monbet, Y., Bassoulet, P., 1989. Bilan des connaissances océanographiques en rade de Brest. Ifremer Scientific report for CEA/IPSN, 89-23, Plouzane (France).
- Nalin, R., Nelson, C.S., Basso, D., Massari, F., 2008. Rhodolith-bearing limestones as transgressive marker beds: fossil and modern examples from North Island, New Zealand. *Sedimentology* 55 (2), 249-274.
- Pardo, C., Guillemain, M.-L., Peña, V., Bárbara, I., Valero, M., Barreiro, R., 2019. Local coastal configuration rather than latitudinal gradient shape clonal diversity and genetic structure of *Phymatolithon calcareum* maerl Beds in north European Atlantic. *Front. Mar. Sci.* 6, 1-9.
- Pears, B., Brown, A.G., Toms, P.S., Wood, J., Sanderson, D., Jones, R., 2020. A sub-centennial-scale optically stimulated luminescence chronostratigraphy and late Holocene flood history from a temperate river confluence. *Geology* 48, 819-825.
- Peña, V., Bárbara, I., 2009. Distribution of the Galician maerl beds and their shape classes (Atlantic Iberian Peninsula): Proposal of areas in future conservation actions. *Cah. Biol. Mar.* 50 (4), 353-368.
- Peña, V., Barreiro, R., Hall-Spencer, J.M., Grall, J., 2013. *Lithophyllum* spp. from unusual maerl beds in the North East Atlantic: the case study of *L. fasciculatum* in Brittany. *An Aod - Les Cahiers Naturalistes de l'Observatoire Marin* 2 (2), 11-21.
- Penaud, A., Ganne, A., Eynaud, F., Lambert, C., Coste, P.O., Herlédan, M., Vidal, M., Goslin, J., Stéphan, P., Charria, G., Pailler, Y., Durand, M., Zumaque, J., Mojtahid, M., 2020. Oceanic versus continental influences over the last 7 kyrs from a mid-shelf record in the northern Bay of Biscay (NE Atlantic). *Quaternary Science Reviews* 229, 106135.
- Petton, S., 2010. Etude des processus hydrodynamiques et hydro-sédimentaires affectant un estran de type marais salé de la rade de Brest (anse de Penfoul) colonisé par l'espèce invasive spartine (*Spartina alterniflora* Loisel). University of Bretagne Occidentale, Brest, (MSC memoir).

- Perry, C.T., 2005. Structure and development of detrital reef deposits in turbid nearshore environments, Inhaca Island, Mozambique. *Mar. Geol.* 214 (1-3), 143-161.
- Poirier C., Tessier B. Chaumillon E., 2017. Climate control on late Holocene high-energy sedimentation along coasts of the northeastern Atlantic Ocean. *Palaeogeogr. Palaeoclimatol. Palaeoecol.* 485, 784-797.
- Poitevin, C., Woppelmann, G., Raucoules, D., Le Cozannet, G., Marcos, M., Testut, L. 2019. Vertical land motion and relative sea-level changes along the coastline of Brest (France) from combined space-borne geodetic methods. *Remote Sens. Environ.* 222, 275-285.
- Pommepey, M., Manaud, F., Monbet, Y., Allen, G., Salomon, J.C., Gentien P., L'Yavang, J., 1979. An oceanographic survey of the bay of Brest S.A.U.M. (Brittany). *Publ. CNEXO (France) Actes Colloq.* 9, 221-226.
- Pouzet, P., Maanan, M., Piotrowska, N., Baltzer, A., Stéphan, P., Robin, M., 2018. Chronology of events along the European Atlantic coasts: New data from the Island of Yeu, France. *Prog. Phys. Geogr.*, 42, (4), 431-450.
- Potin, P., Floch, J.Y., Augris, J., Cabioch, J., 1990. Annual growth rate of calcareous red alga *Lithothamnion corallioides* (Corallinales, Rhodophyta) in the Bay of Brest, France. *Hydrobiologia* 204 (1), 263-267.
- Ragueneau, O., Raimonet, M., Mazé, C., Coston-Guarini, F., Chauvaud, L., Danto, A., Grall, J., Jean, F., Paulet, Y.M., Thouzeau, G., et al., 2018. The Impossible Sustainability of the Bay of Brest? Fifty Years of Ecosystem Changes, Interdisciplinary Knowledge Construction and Key Questions at the Science-Policy-Community Interface. *Front. Mar. Sci.* 5, 124. <https://doi.org/10.3389/fmars.2018.00124>.
- Regnaud, H., Jennings, S., Delaney, C., Lemaçon L., 1996. Holocene sea-level variations and geomorphological response: an example in Northern Brittany. *Quat. Sci. Rev.* 15 (8-9), 781-787.
- Reimer, P.J., Bard, E., Bayliss, A., Beck, J.W., Blackwell, P.G., Bronk Ramsey, C., Buck, C.E., Cheng, H., Edwards, R.L., Friedrich, M., Grootes, P.M., Guilderson, T.P., Haffliger, H., Hajdas, I., Hatté, C., Heaton, T.J., Hoffman, D.L., Hogg, A.G., Hughen, K.A., Kaiser, K.F., Kromer, B., Manning, S.W., Niu, M., Reimer, R.W., Richards, D.A., Scott, E.M., Southon, J.R., Staff, R.A., Turney, C.S.M., Van der Plicht, J., 2013. IntCal13 and Marine13 radiocarbon age calibration curves 0-50,000 years cal B.P. *Radiocarbon* 55 (4), 1869-1887.
- Riul, P., Targino, C.H., Farias, J.D.N., Visscher, P.T., Horta, P.A., 2008. Decrease in *Lithothamnion* sp. (Rhodophyta) primary production due to the deposition of a thin sediment layer. *J. Mar. Biol. Assoc. U. K.* 88 (1), 17-19.
- Roberts, N., Fyfe, R.M., Woodbridge, J., Gaillard, J.M., Davis, B.A.S., Kaplan, J.O., Marquer, L., Mazier, F., Nielsen, A.B., Sugita, S., Trondman, A.-K., Leydet, M., 2018. Europe's lost forests: a pollen-based synthesis for the last 11,000 years. *Sci. Rep.* 8, 1-8.
- Sarkar, S., 2017. Ecology of Coralline Red Algae and Their Fossil Evidences from India. *Thalassas* 33, 15-28.

- Sekanina, L., Harding, S.L., Banzhaf, W., Kowaliw, T., 2011. Image processing and CGP, in: Miller, J.F. (Eds.), Cartesian Genetic Programming. Natural Computing Series, Springer publisher, pp.181-215
- Sorrel, P., Debret, M., Billeaud, I., Jaccard, S.L., McManus, J.F., Tessier, B., 2012. Persistent non-solar forcing of Holocene storm dynamics in coastal sedimentary archives. *Nat. Geosci.* 5 (12), 892-896.
- Steller, D.L., Foster, M.S., 1995. Environmental factors influencing distribution and morphology of rhodoliths in Bahía Concepción, B.C.S., México. *J. Exp. Mar. Biol. Ecol.* 194 (2), 201-212.
- Steller, D.L., Hernandez-Ayon, J.M., Riosmena-Rodriguez, R., Cabello-Pasini, A., 2007. Effect of temperature on photosynthesis, growth and calcification rates of the free-living coralline alga *Lithophyllum margaritae*. *Cienc Mar* 33 (4), 441-456.
- Stéphan, P., 2008. Les flèches de galets de Bretagne: morphodynamiques passée, présente et prévisible Géomorphologie. University of Bretagne Occidentale, Brest, France (PhD thesis).
- Stéphan, P., Fichaut B., Suanez, S., 2005. Les cordons littoraux de Mengleuz (Logonna-Daoulas) et du Loc'h de Landévennec: aspects récents et actuels de l'érosion de deux flèches de galets en rade de Brest. *Bull. Soc. géol. minéral. Bretagne* (2), 1-19.
- Stéphan, P., Goslin, J., Pailler, Y., Manceau, R., Sanchez, S., Van Vliet-Lanoë, B., Hénaff, A., Delacourt, C., 2015. Holocene salt-marsh sedimentary infilling and relative sea-level changes in West Brittany (France) using foraminifera-based transfer functions. *Boreas* 44 (1), 153-177.
- Stuiver, M., Reimer, P.J., 1993. Extended ^{14}C Data Base and Revised CALIB 3.0 ^{14}C Age Calibration Program. *Radiocarbon* 35, 215-230. CALIB Rev 7.1.
- Tabeaud, M., Lysaniuk, B., Schoenewald, N., Buridant, J., 2009. Le risque « coup de vent » en France depuis le XVI^e siècle, in : Armand Colin (Eds), *Annales de géographie* 3 (667), pp.318-331.
- Teichert, S., Woelkerling, W., Rüggeberg, A., Wisshak, M., Piepenburg, D., Meyerhöfer, M., Form, A., Büdenbender, J., Freiwald, A., 2012. Rhodolith beds (Corallinales, Rhodophyta) and their physical and biological environment at 80°31'N in Nordkappbukta (Nordaustlandet, Svalbard Archipelago, Norway). *Phycologia* 51 (4), 371-390.
- Tessier, B., Billeaud, I., Sorrel P., Delsinne, N., Lesueur, P., 2012. Infilling stratigraphy of macrotidal tide-dominated estuaries. Controlling mechanisms: Sea level fluctuations, bedrock morphology, sediment supply and climate changes (The examples of the Seine estuary and the Mont-Saint-Michel Bay, English Channel, NW France). *Sediment. Geol.* 279, 62-73.

- Tisnérat-Laborde, N., Paterne, M., Métivier, B., Arnold, M., Yiou, P., Blamart, D., Raynaud, S., 2010. Variability of the northeast Atlantic sea surface $\Delta 14\text{C}$ and marine reservoir age and the North Atlantic Oscillation (NAO). *Quat. Sci. Rev.* 29 (19-20), 2633-2646.
- Travers, M.A., Basuyaux, O., Le Goïc, N., Huchette, S., Nicolas, J.L., Koken, M., Paillard, C., 2009. Influence of temperature and spawning effort on *Haliotis tuberculata* mortalities caused by *Vibrio harveyi*: an example of emerging vibriosis linked to global warming. *Glob. Chang. Biol.* 15 (6), 1365-1376.
- Tréguer, P., Goberville, E., Barrier, N., L'Helguen, S., Morin, P., Bozec, Y., Rimmelín-Maury, P., Czamanski, M., Grossteffan, E., Cariou, T., Répécaud, M., Quémener, L., 2014. Large and local-scale influences on physical and chemical characteristics of coastal waters of Western Europe during winter. *J. Mar. Syst.* 139, 79-90.
- Troadec, P., Le Goff, R., 1997. Etat des lieux et des milieux de la rade de Brest et de son bassin versant. Phase Préliminaire du Contrat Baie Rade Brest. Edition Communauté Urbaine de Brest.
- Qui-Minet, Z.M., Delaunay, C., Grall, J., Six, C., Cariou, T., Boime, O., Legrand, E., Davoult D., Martin S., 2018. The role of local environmental changes on maerl and its associated non-calcareous epiphytic flora in the Bay of Brest. *Estuar. Coast. Shelf. Sci.* 208, 140-152.
- Vale, N.F.L., Amado-Filho, G.M., Braga, J.C., Bracelenho, P.S., Karez, C.S., Moraes, F.C., Bahia, R.G., Bastos, A.C., Moura, R.L., 2018. Structure and composition of rhodoliths from the Amazon River mouth, Brazil. *Journal of South American Earth Sciences* 84, 149-159.
- Van Geel, B., Buurman, J., Waterbolk, H.T., 1996. Archaeological and palaeological indications of an abrupt climate change in The Netherlands, and evidence for climatological teleconnections around 2650 B.P. *J. Quat. Sci.* 11 (6), 451-460.
- Van Vliet-Lanoë, B., Goslin, J., Hallégouët, B., Hénaff, A., Delacourt, C., Fernane, A., Franzetti, M., Le Cornec, E., Le Roy, P., Penaud, A., 2014a. Middle- to late-Holocene storminess in Brittany (NW France): Part I - morphological impact and stratigraphical record. *Holocene* 24 (4), 413-433.
- Van Vliet-Lanoë, B., Penaud, A., Hénaff, A., Delacourt, C., Fernane, A., Goslin, J., Hallégouët, B., Le Cornec, E., 2014b. Middle- to late-Holocene storminess in Brittany (NW France): Part II – The chronology of events and climate forcing. *Holocene* 24 (4), 434-453.
- Van Vliet-Lanoë, B., Goslin, J., Hénaff, A., Hallégouët, B., Delacourt, C., Le Cornec, E., Meurisse-Fort, M., 2016. Holocene formation and evolution of coastal dunes ridges, Brittany (France). *C. R. Geosci.* 348 (6), 462-470.

- Villas-Boas, A.B., Tâmega, F.T.S., Coutinho, M.A.R., Figueiredo, M.A.O., 2014. Experimental effects of sediment burial and light attenuation on two coralline algae of a deep water rhodolith bed in Rio de Janeiro, Brazil. *Cryptogam Algal* 35 (1), 67-76.
- Wang, T., Surge, D., Mithen, S., 2012. Seasonal temperature variability of the Neoglacial (3300–2500 B.P.) and Roman Warm Period (2500–1600 B.P.) reconstructed from oxygen isotope ratios of limpet shells (*Patella vulgata*), Northwest Scotland. *Palaeogeogr. Palaeoclimatol. Palaeoecol.* 317-318, 104-113.
- Wanner, H., Beer, J., Bütikofer, J., Crowley, T.J., Cubasch, U., Flückiger, J., Goosse, H., Grosjean, M., Joos, F., Kaplan, J.O., Küttel, M., Müller, S.A., Prentice, I.C., Solomina, O., Stocker, T.F., Tarasov, P., Wagner, M., Widmann, M., 2008. Mid-to Late Holocene climate change: an overview. *Quat. Sci. Rev.* 27 (19-20), 1791-1828.
- Wanner, H., Solomina, O., Grosjean, M., Ritz, S.P., Jetel, M., 2011. Structure and origin of Holocene cold events. *Quat. Sci. Rev.* 30 (21-22), 3109-3123.
- WASA Group, 1998. Changing Waves and Storms in the Northeast Atlantic? *Bull. Am. Meteorol. Soc.* 79 (5), 741-760.
- Wehrmann, A., 1998. Modern cool-water carbonates on a coastal platform of northern Brittany, France: Carbonate production in macrophytic systems and sedimentary dynamics of bioclastic facies. *Senckenbergiana maritima* 28 (4-6), 151-166.
- Williams, M., 2003. *Deforesting the Earth: from Prehistory to Global Crisis*, University of Chicago Press.
- Wilson, S., Blake, C., Berges, J.A., Maggs, C.A., 2004. Environmental tolerances of free-living coralline algae (maerl): implications for European marine conservation. *Biol. Conserv.* 120 (2), 279-289.
- Yang, X., Cai, X., Maslov, K., Wang, L., Luo, Q., 2010. High-resolution photo acoustic microscope for rat brain imaging in vivo. *Chin. Opt. Lett.* 8 (6), 609-611.
- Ziegler, P.A., 1992. European Cenozoic rift system, in: Ziegler, P.A. (Eds), *Geodynamics of Rifting*. Volume 1. Case History Studies on Rifts: Europe and Asia. *Tectonophysics* 208, 91-111.

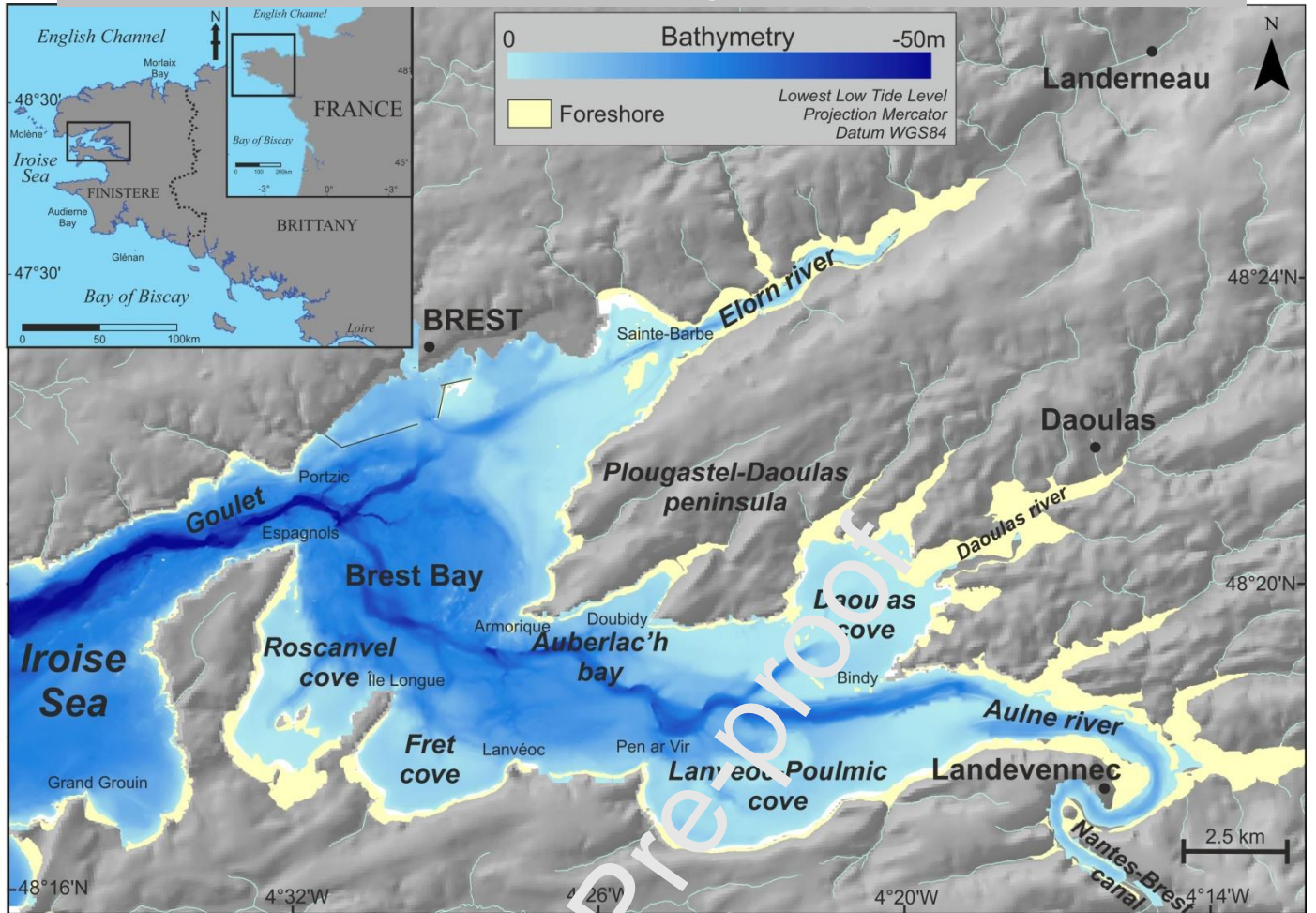


Figure 1: Geographical (© BDalt) and bathymetric (Gregoire et al., 2016) settings of the Bay of Brest (BB).

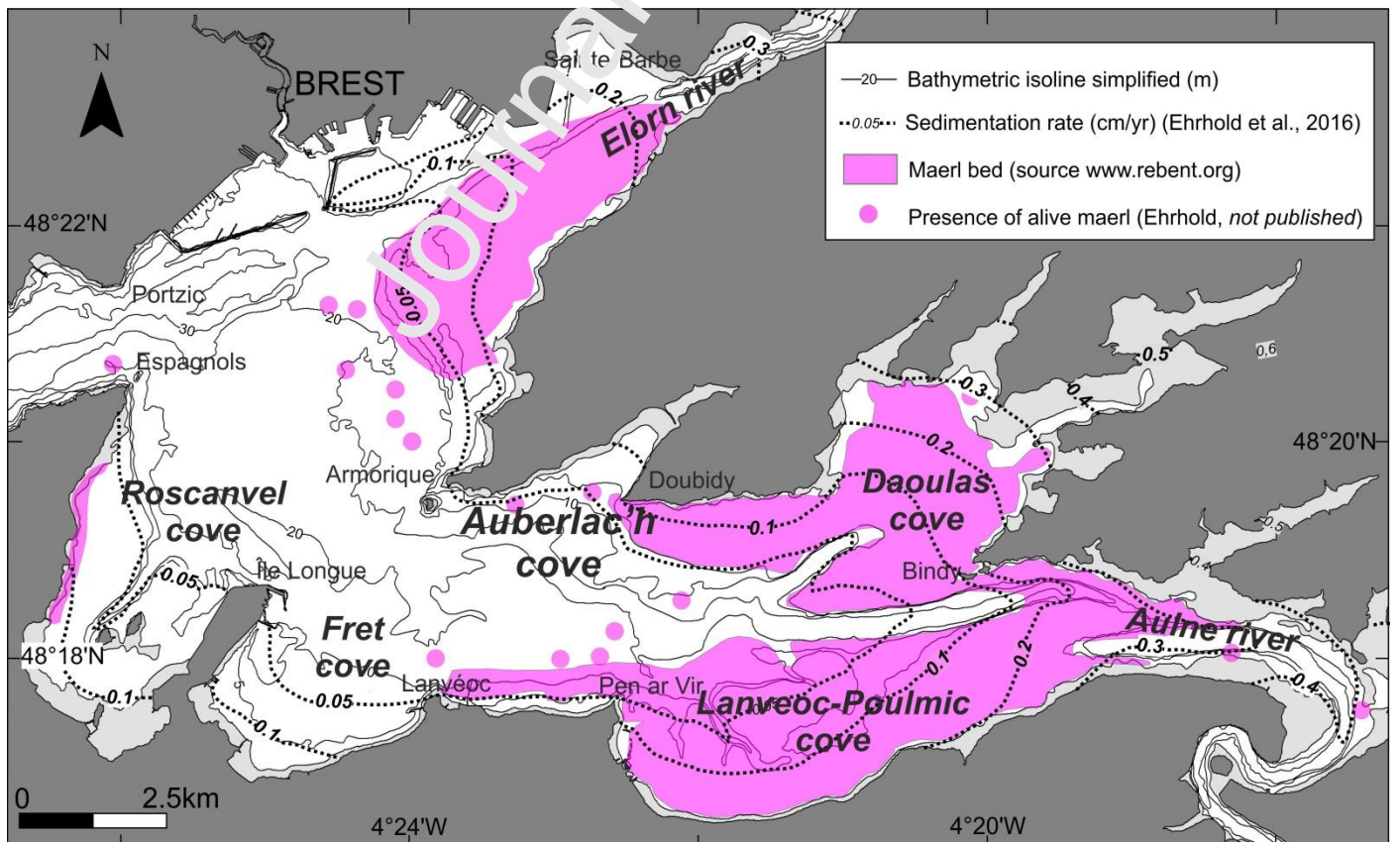


Figure 2: Modern sedimentation rates (modified from Ehrhold et al., 2016) and maerl bed deposits in the Bay of Brest.

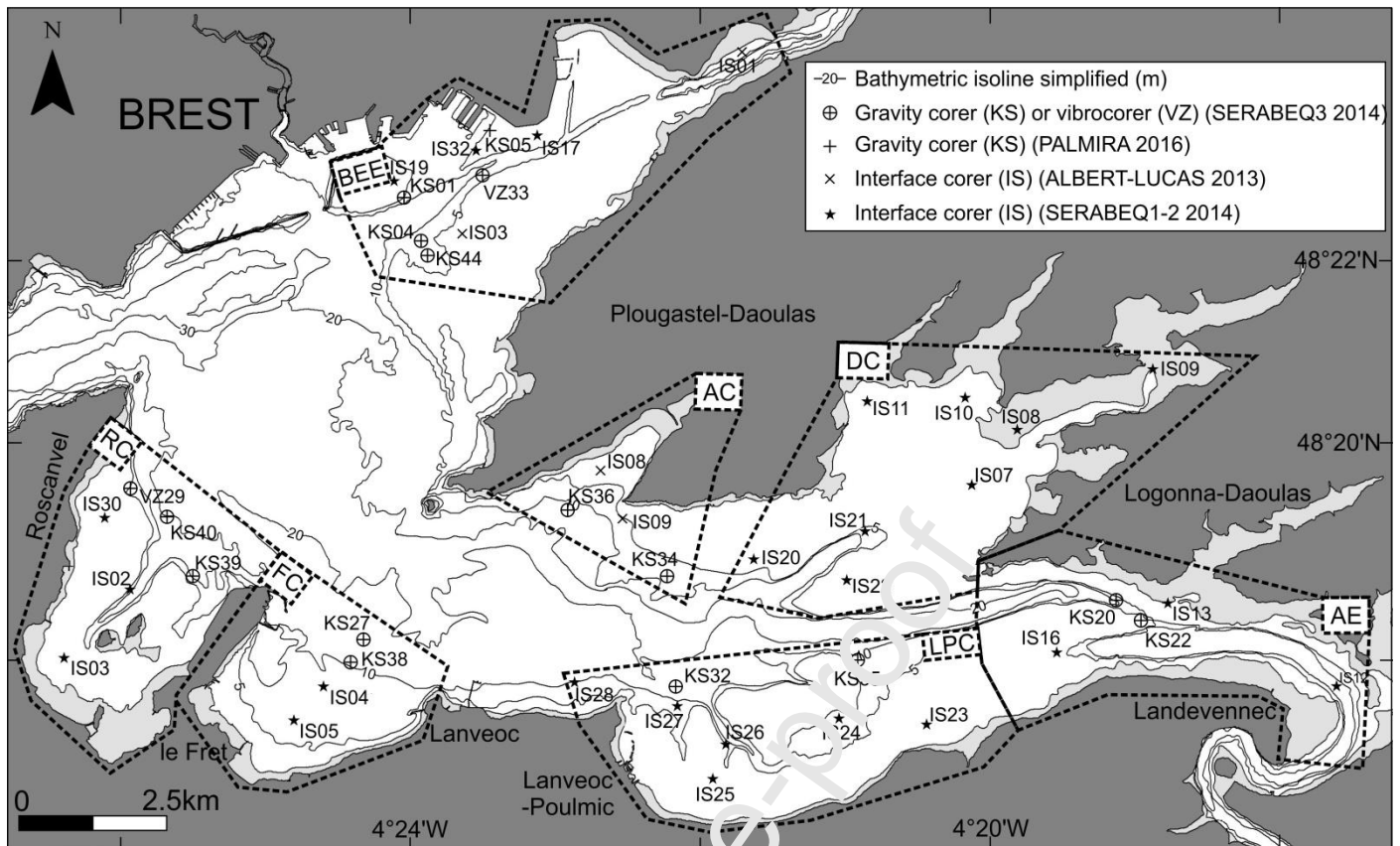


Figure 3: Location of sediment cores (KS) and interface cores (IS) used in this study (RC: Roscanvel cove; FC: Fret cove; LPC: Lanvéoc-Poulmic cove; AE: Aune estuary; DC: Daoulas cove; AC: Auberlac'h cove; BEE: Brest-Elorn estuary).

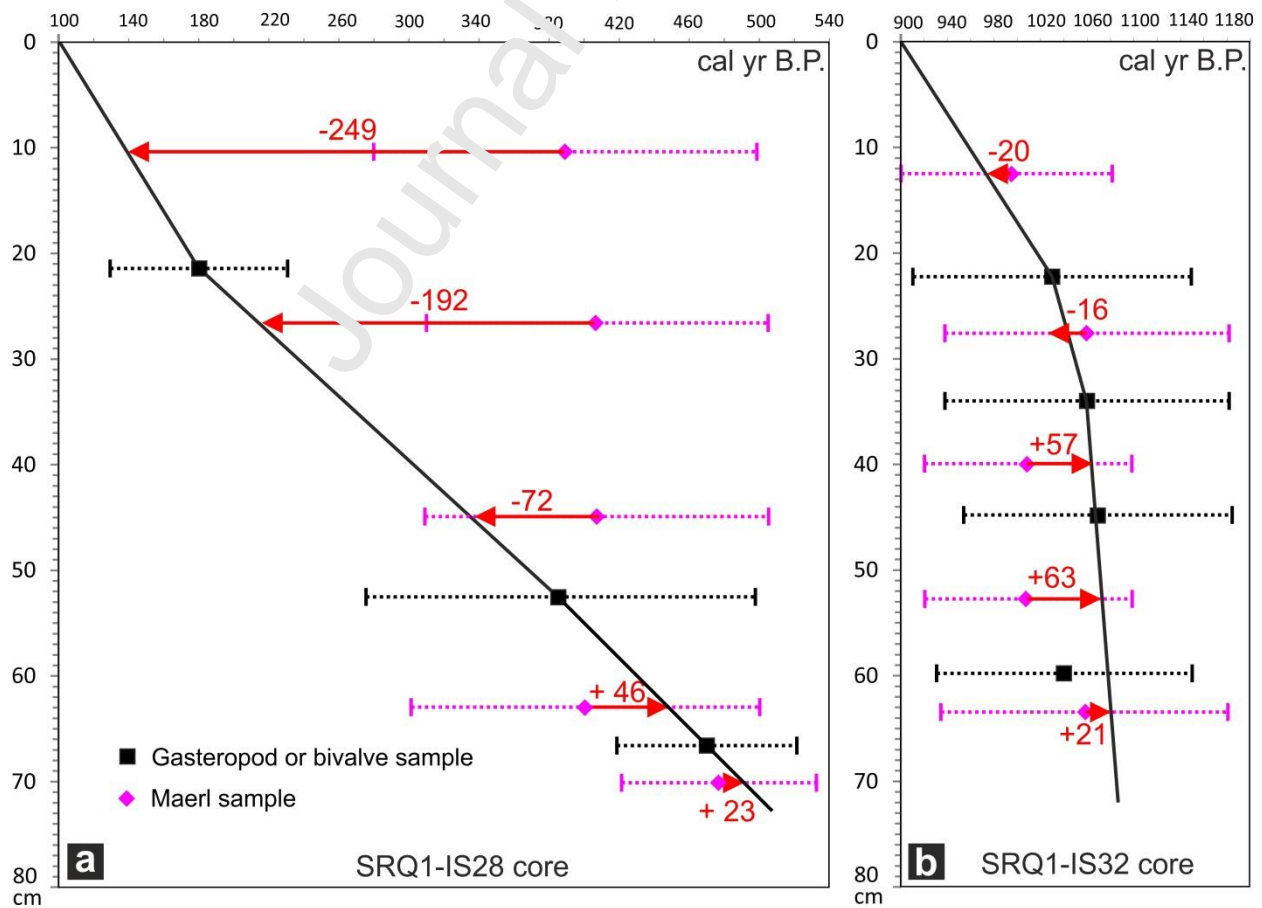


Figure 4: Drift (red arrow) and uncertainties (dashed point) on the ^{14}C ages obtained on maerl thalli and compared with mollusk samples in two age-depth models (a: SRQ1-IS28; b: SRQ1-IS32).

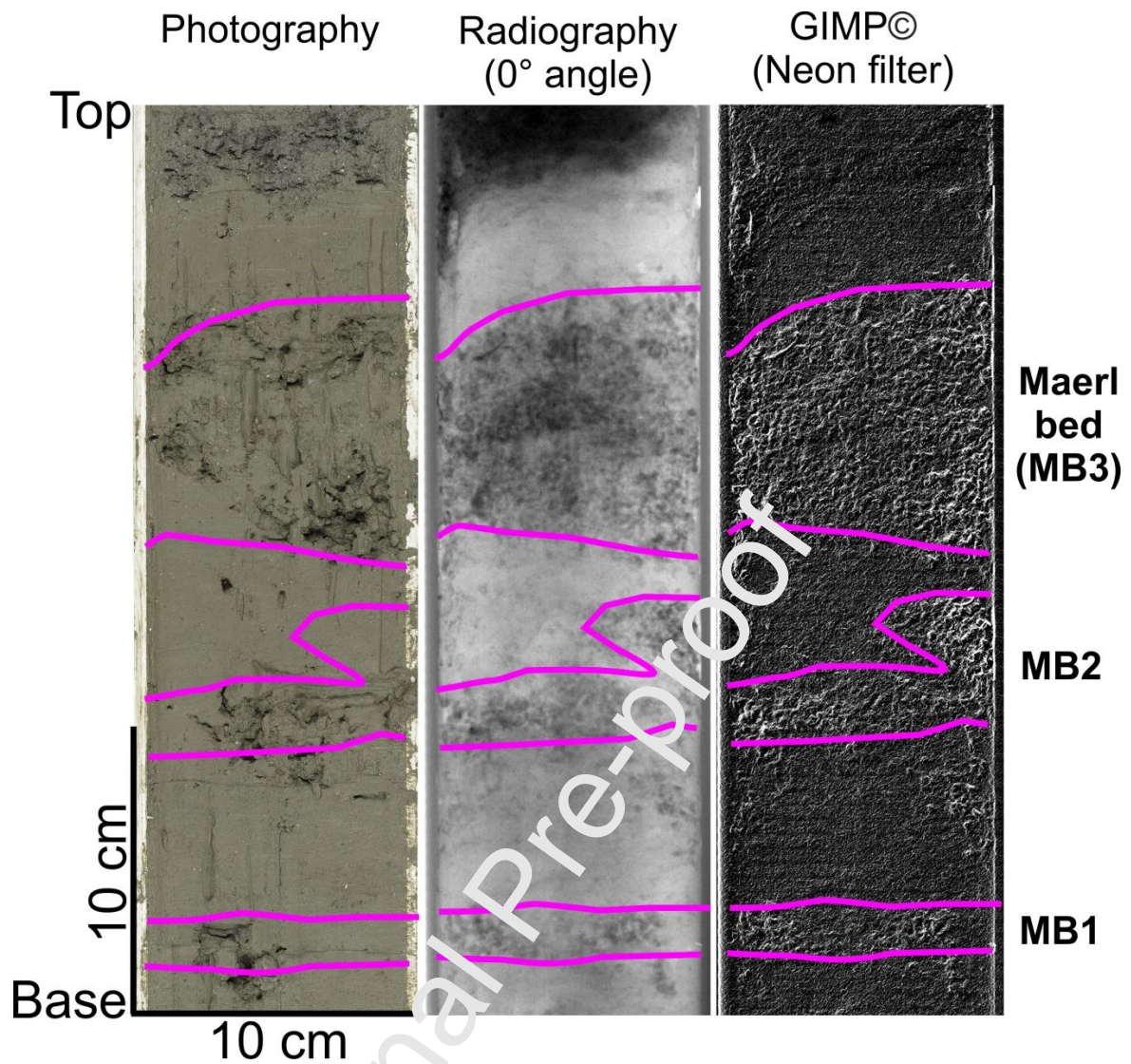


Figure 5: Methodology used within the study to detect fossil maerl beds (example of core SRQ3-KS34-38-68cm).

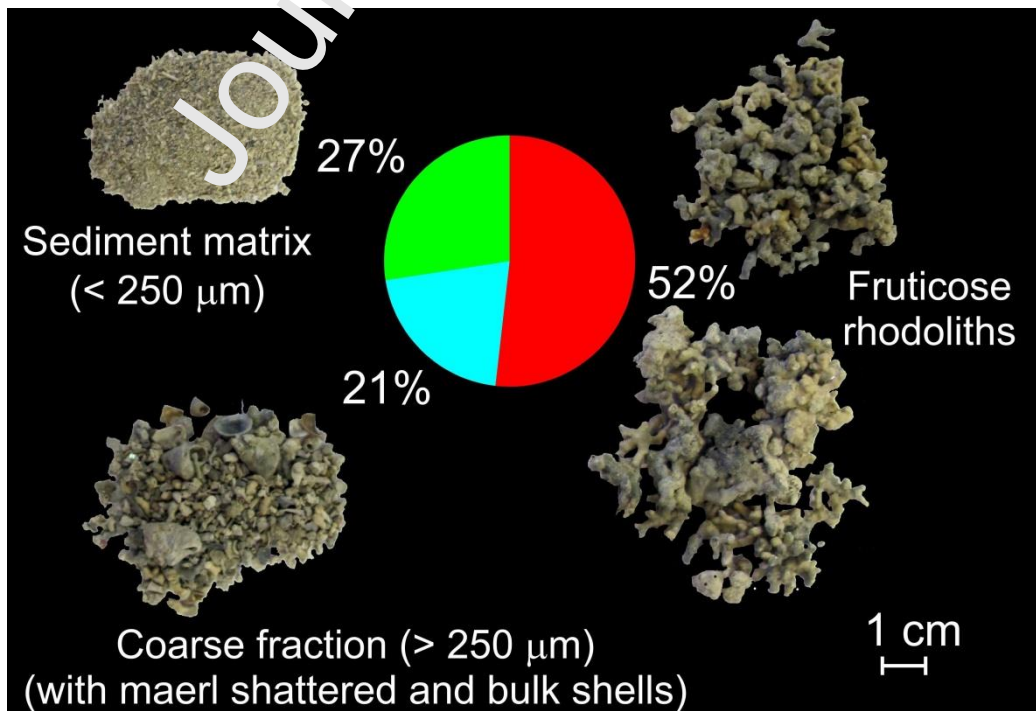


Figure 6: Example of the extraction of different granulometric fractions to define percentage of unaltered maerl bed and associated sedimentary fractions.

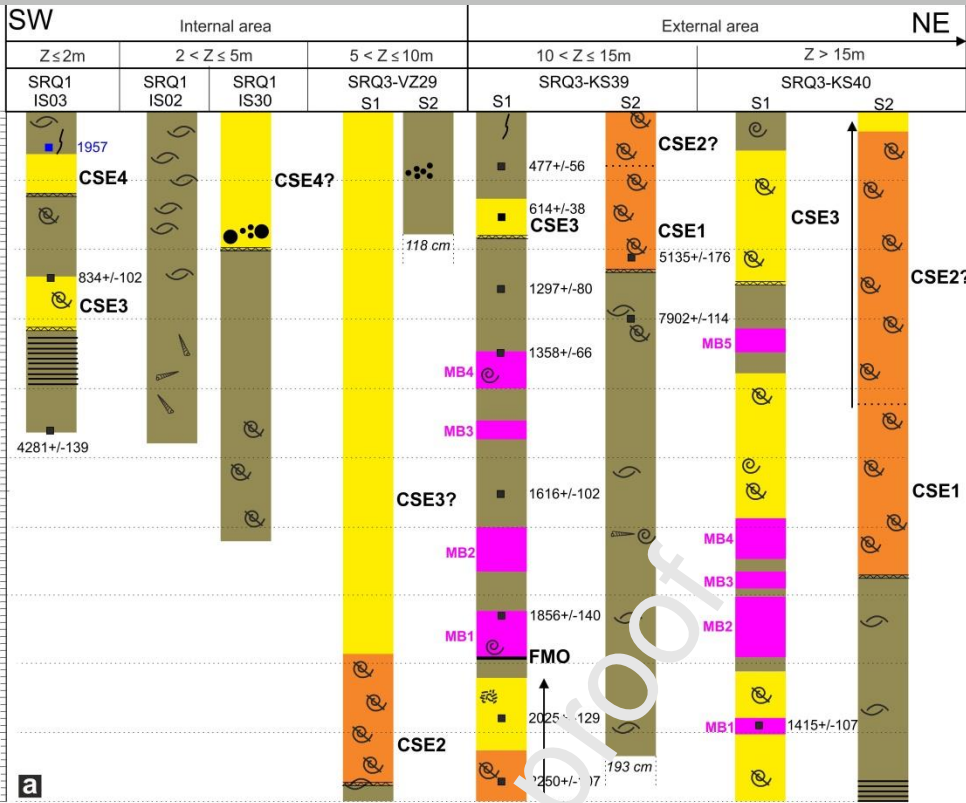


Figure 7: Synthetic lithological descriptions of selected gravity cores in Roscanvel cove (a) and Le Fret cove (b)

(see figure 3 for geographical location of cores).

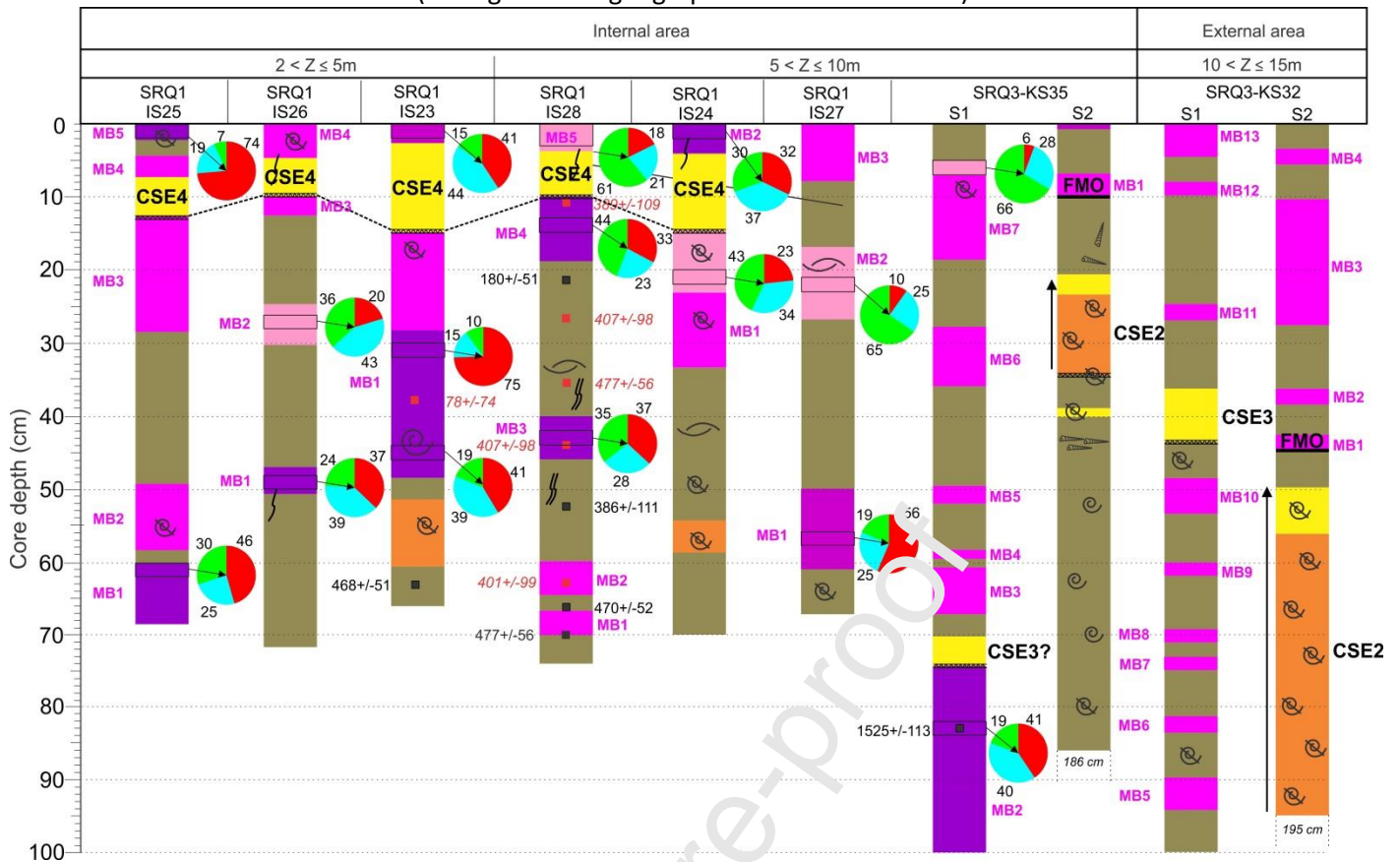


Figure 8: Synthetic lithological descriptions of collected gravity cores in Lanveoc-Poulmic cove (see figure 7 for the legend and figure 3 for geographical location of cores).

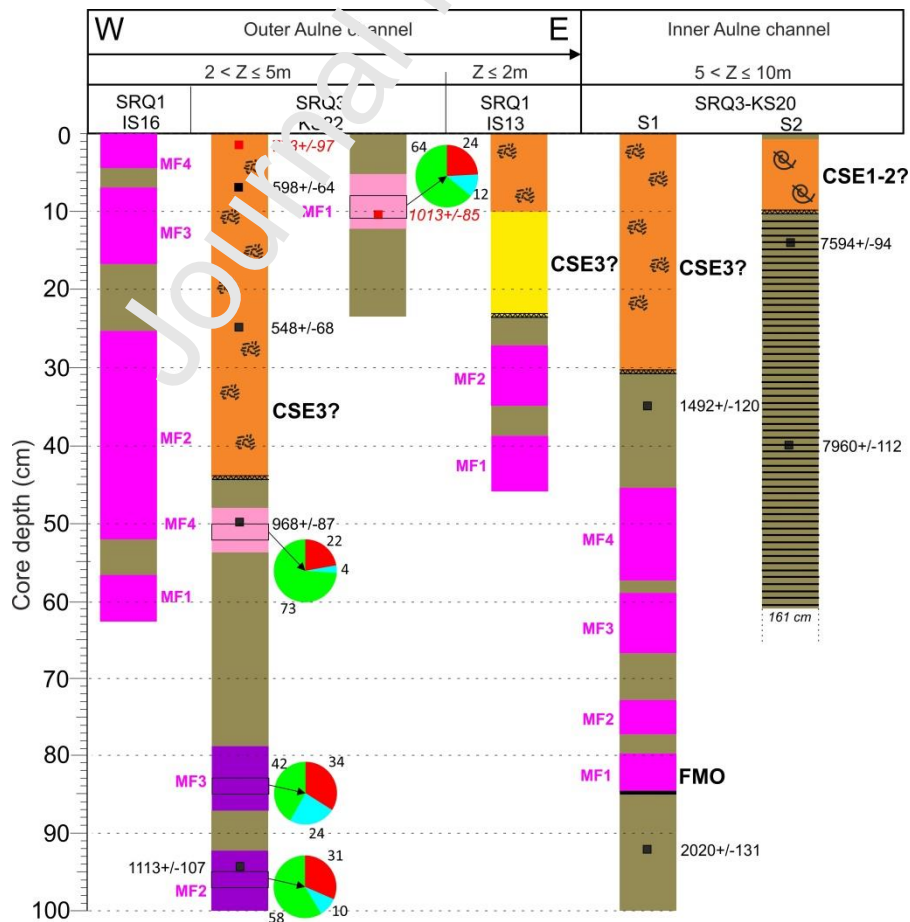
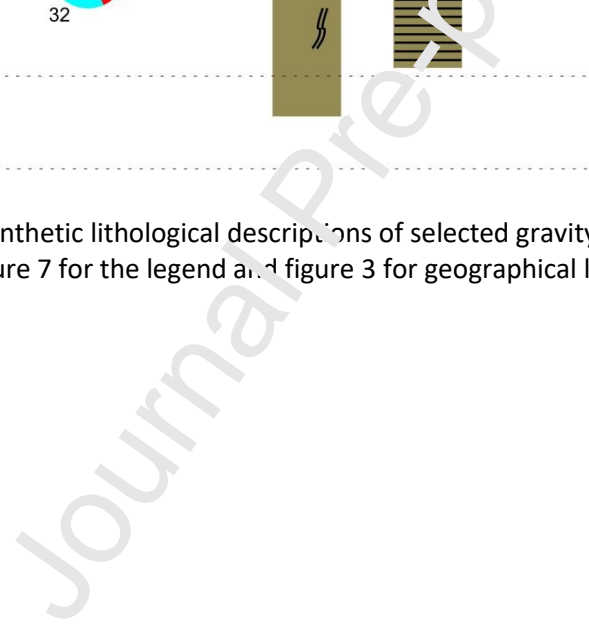


Figure 9: Synthetic lithological descriptions of selected gravity cores in Aulne estuary



(see figure 7 for the legend and figure 3 for geographical location of cores).

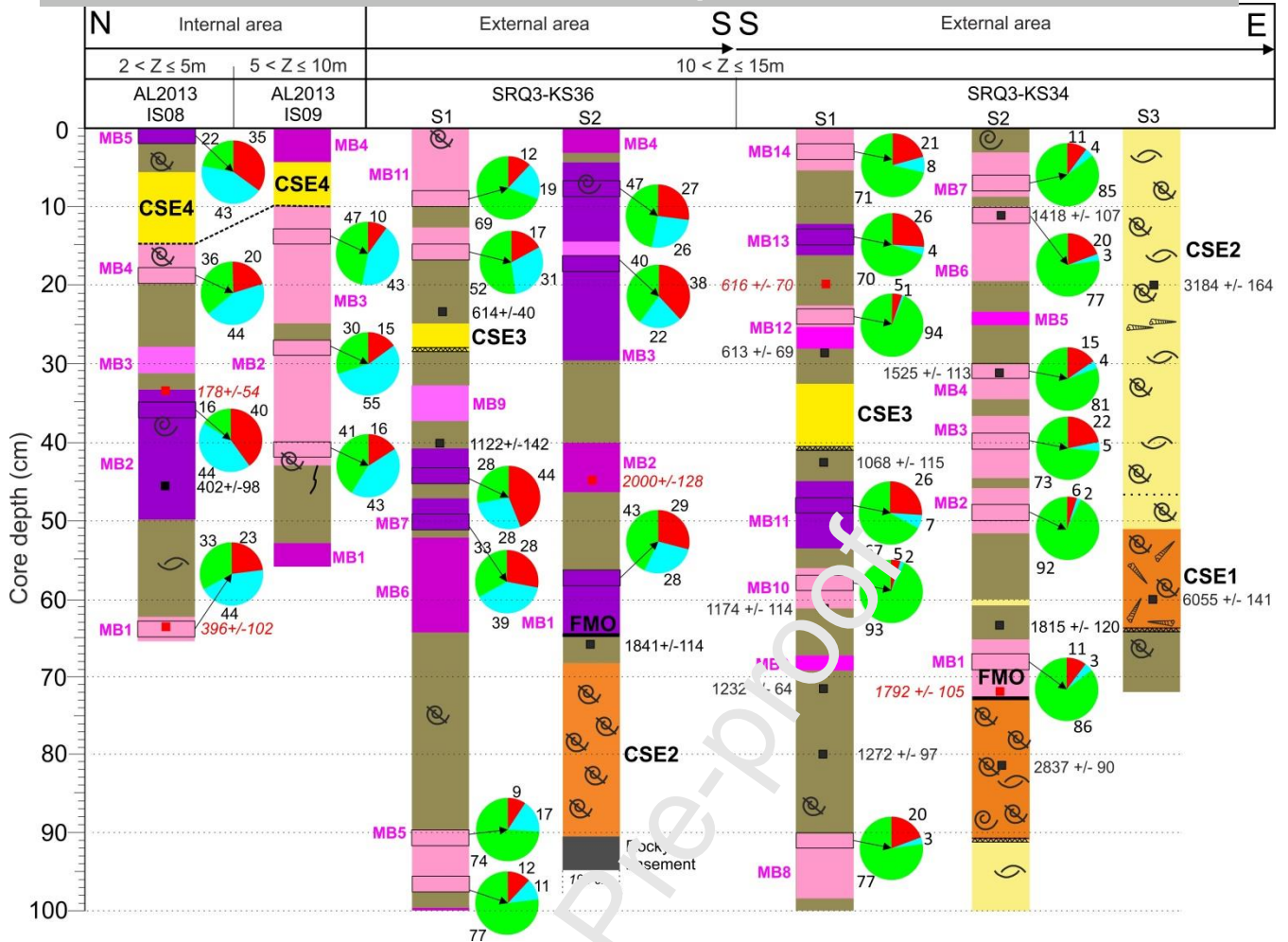


Figure 11: Synthetic lithological descriptions of selected gravity cores in Auberlac'h cove

(see figure 7 for the legend and figure 3 for geographical location of cores).

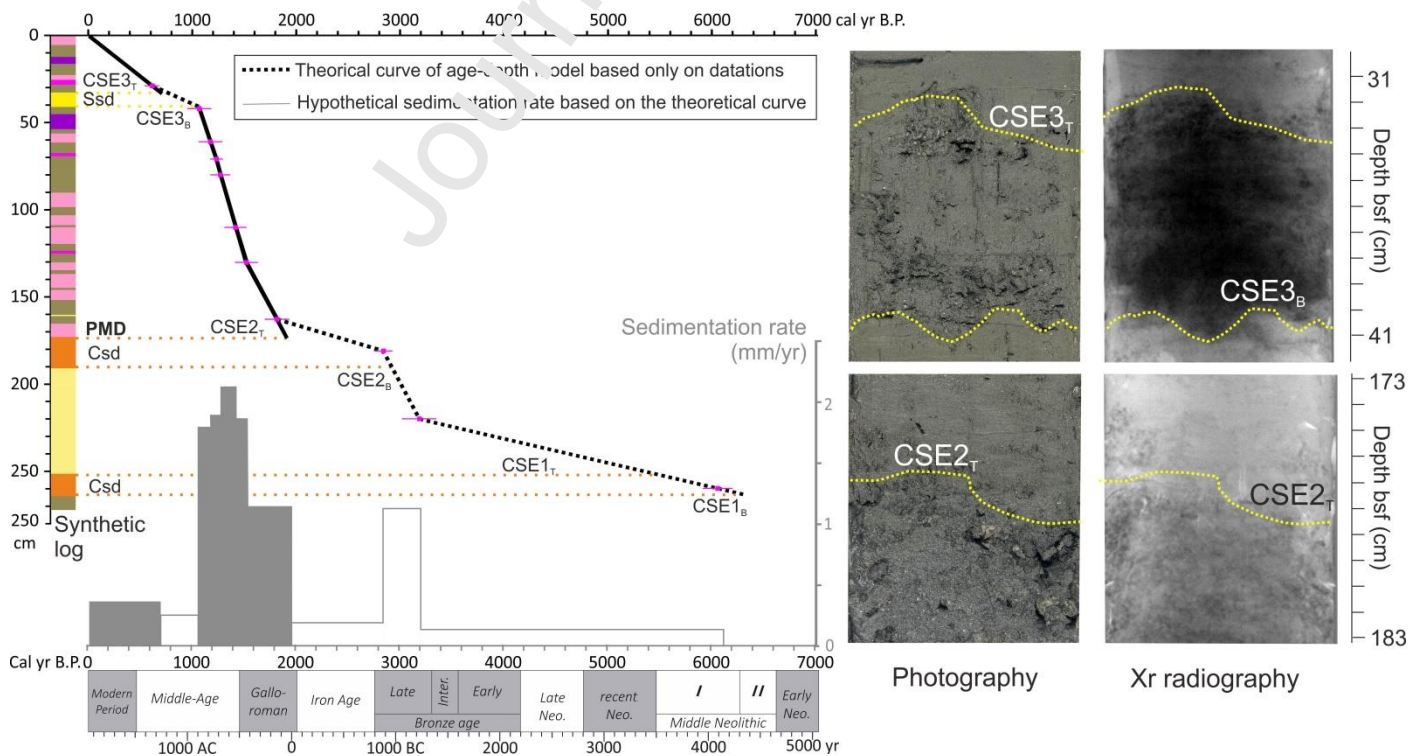


Figure 12: Age-depth model for external part of Auberlac'h bay (SRQ3-KS34 core) and imagery evidence

of major *hiatus* limits (CSE1, 2 and 3). FMO: First maerl occurrence; Ssd: Sand sedimentary deposit; Csd: Coarse sedimentary deposit. Synthetic log of core SRQ3-KS34 (Fig. 11).

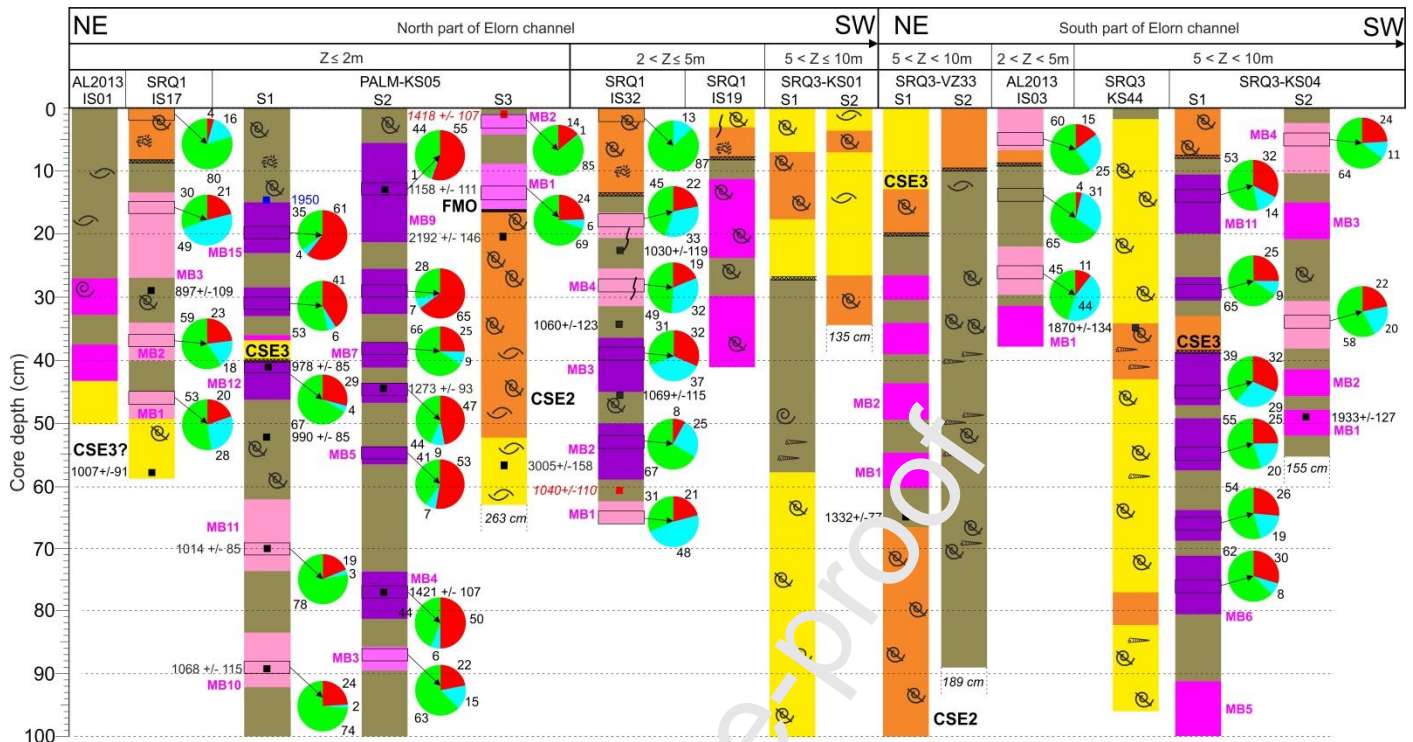


Figure 13: Synthetic lithological descriptions of selected gravity cores in Brest-Elorn estuary (see figure 7 for the legend and figure 3 for geographical location of cores).

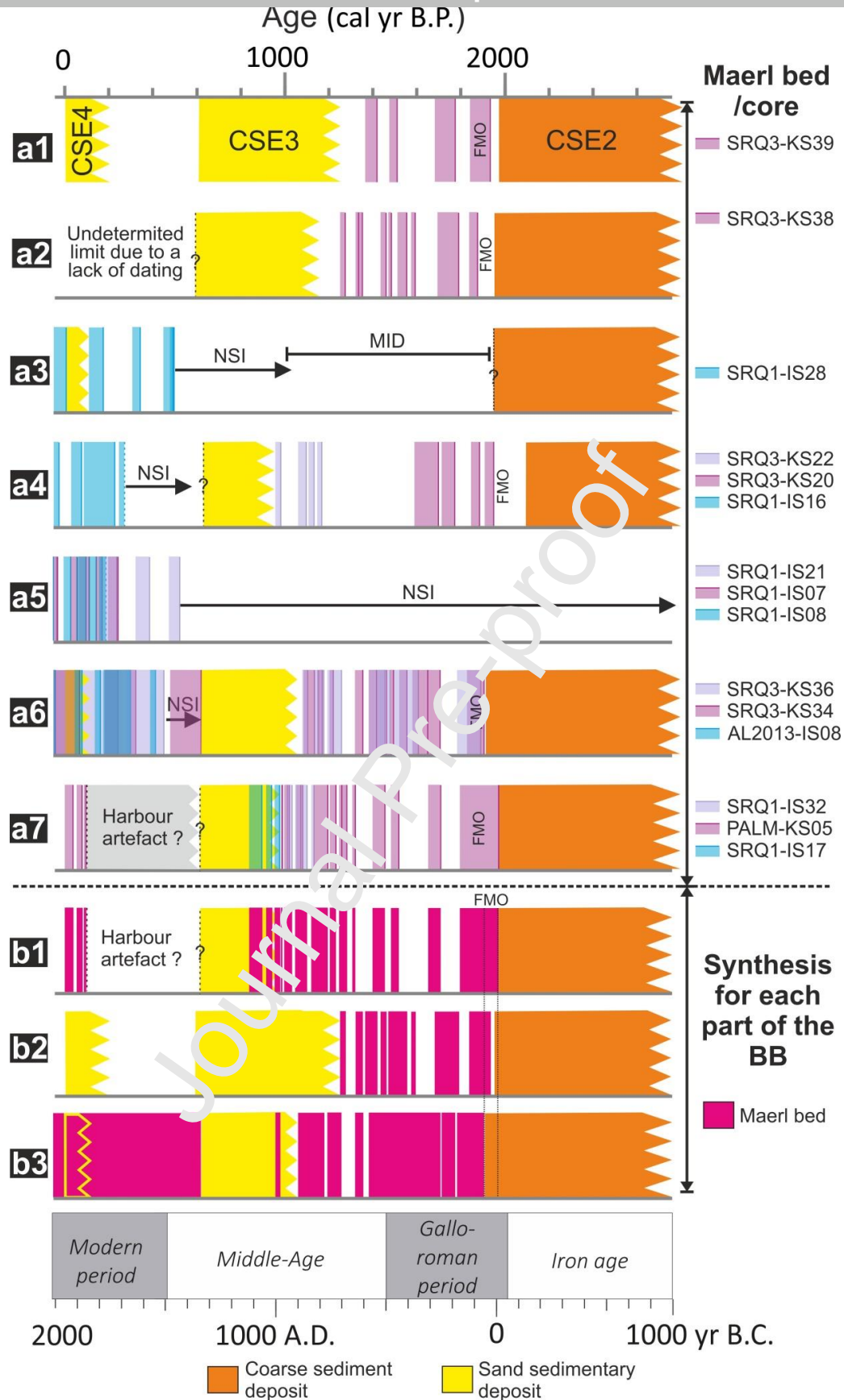


Figure 14: Position of fossil maerl beds and sedimentary crises over the last 3000 years for (a) each sector of the Bay of Brest (1: RC; 2: FC; 3: LPC; 4: AE; 5: DC; 6: AC; 7: BEE) and (b) synthesis of all fossil maerl beds for each main domain of the BB (1: inner Elorn estuary (northern BB); 2: outer Aulne estuary (southern BB); 3: inner Aulne estuary

(southern BB). MID: Presence of maerl bed but insufficient Dating; NSI: No Sedimentary Information in shallow water

depth $Z < 5$ m; FMO: First maerl occurrence; CSE: Coarse Sedimentary Events).

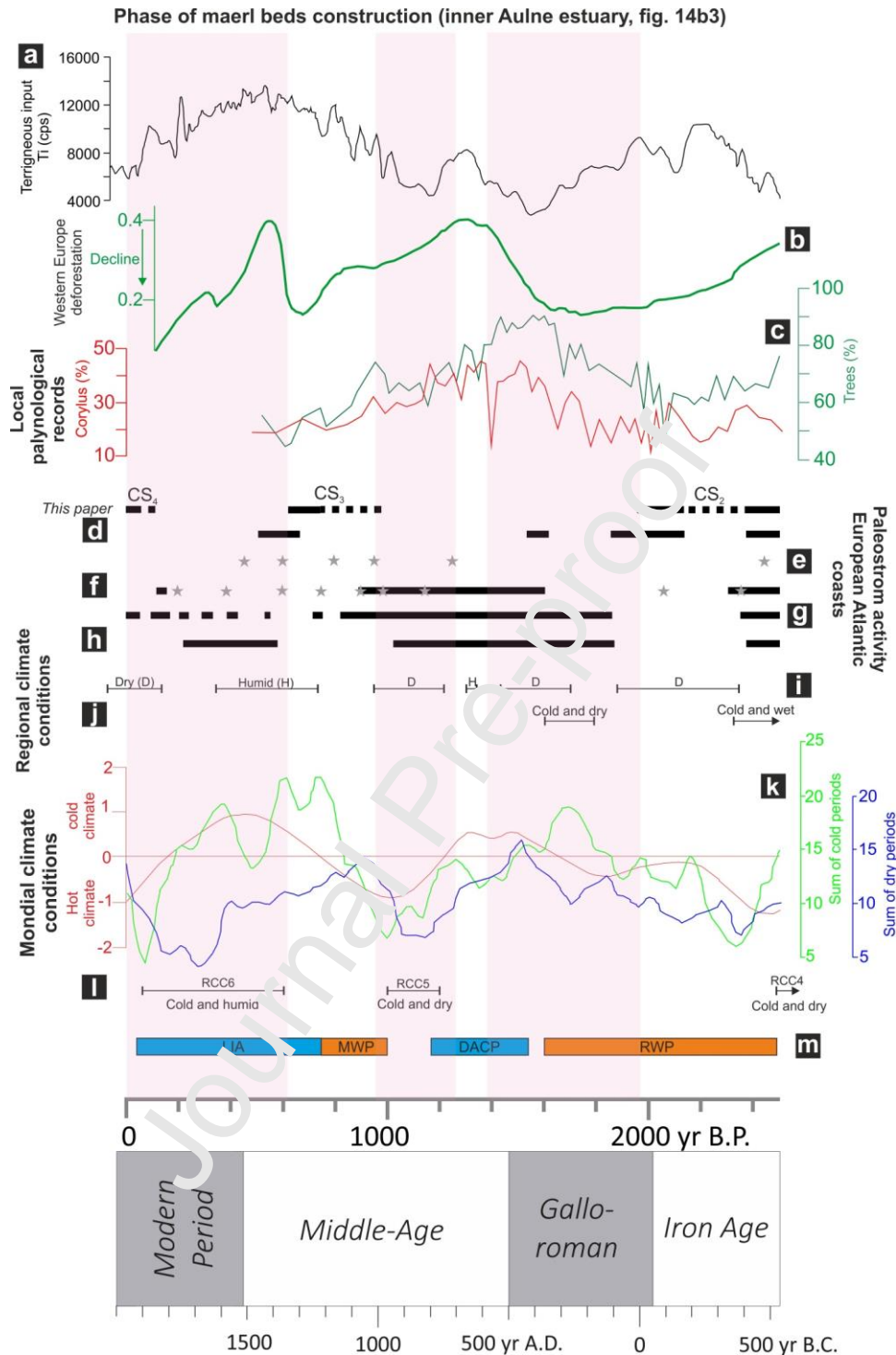


Figure 15: The main phases of maerl bed construction (illustrated by pink bands) compared with a selection of global and regional proxies, and displayed in cal. yr B.P. (upper scale) and AD/BC (lower scale): a - Terrigenous input for Loire estuary (Durand et al., 2018). b - Western Europe deforestation (Kaplan et al., 2009). c - Local palynological records (Lambert et al., 2020). d.h - Paleostorm activity (grey star for event and solid line for period) on European Atlantic coasts (d, Pouzet et al., 2018; e, Poirier et al., 2017; f, Van Vliet-Lanoë et al., 2014 and 2016; g, Durand et al., 2018; h, Sorrel et al., 2012). i-j - Regional climate conditions (i, Durand et al., 2018; j, Fernane et al., 2014; Goslin, 2014). k-l - Global climate conditions (k, Wanner et al., 2011; l, Rapid Climate Change (RCC) for Mayewski et al.,

2004). M – Climatic periods (LIA, Ilyashuk et al., 2019; MWP, Helama et al., 2009; DACP, Helama et al., 2017; RWP, Wang et al., 2012).

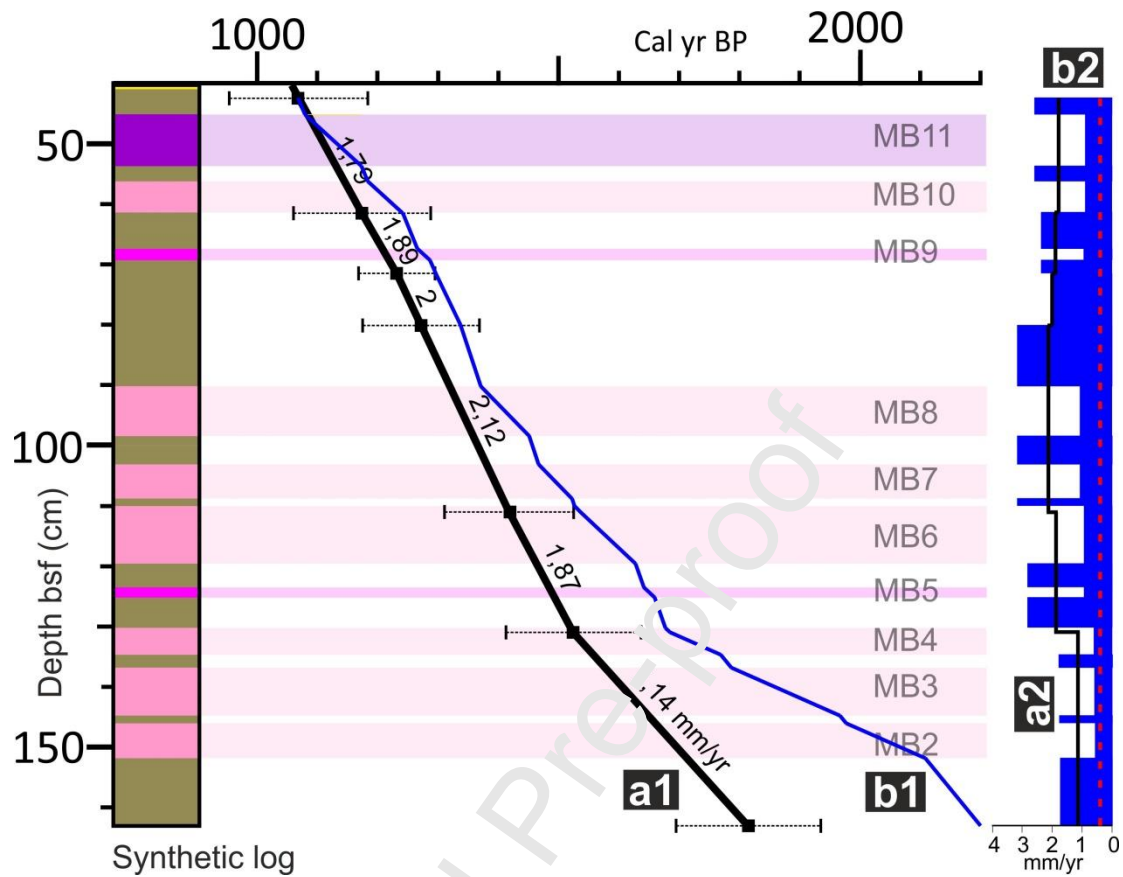


Figure 16: a1: Sedimentation rates and maerl bed development (a1: age-depth model (black line) for the SRQ3-KS34 core section limited between 40 to 160 cm bsf (extracted from Fig. 12); b1: Theoretical age-depth model (blue line) for 50% reduction of local sedimentation rate during maerl bed development; a2: Sedimentation rates based on a1; b2: sedimentation rates based on b1). Red dashed line: modern sedimentation rate (Ehrhold et al., 2016, Fig. 2). MB: maerl bed facies.

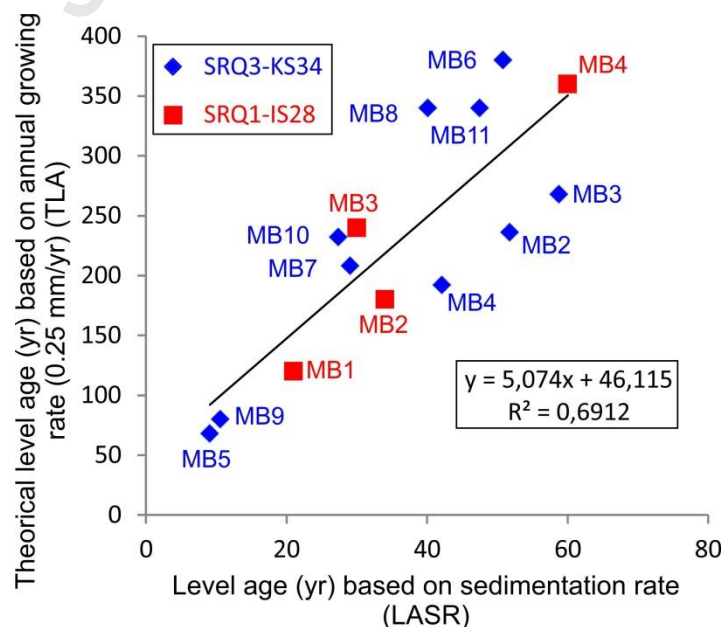


Figure 17: Comparison of maerl bed ages based on sedimentation rates and annual growth for SRQ3-KS34 (40-160 cm bsf, see Fig. 16) and SRQ1-IS28 cores (10-70 cm bsf).

Sites in the Bay of Brest	Sample and lab. no.	Core depth (cm)	Altitude LLTL (m)	AMS ¹⁴ C ages (radiocarbon yr B.P.)	Calibrated aged cal yr B.P. (mean) (2σ)	Age cal (A.D./B.C.)	Dated material	References
Roscanvel	SRQ1-IS03 (Beta-397592)	24	-1.8	1260 ± 30	937 - 732 (835)	1013 - 1218 (A.D.)	Molluscs	
Roscanvel	SRQ1-IS03 (Poz-65763)	46-47	-1.8	4175 ± 35	4420 - 4141 (4282)	2471 - 2192 (B.C.)	Molluscs	
Roscanvel	SRQ3-KS39 (Poz-76861)	8	-11.5	740 ± 30	533 - 421 (477)	1417 - 1529 (A.D.)	Molluscs	Gregoire et al. (2017)
Roscanvel	SRQ3-KS39 (Beta-468466)	15-16	-11.5	880 ± 30	653 - 576 (615)	1297 - 1374 (A.D.)	Molluscs	
Roscanvel	SRQ3-KS39 (Beta-468467)	25-26	-11.5	1690 ± 30	1378 - 1217 (1298)	572 - 733 (A.D.)	Molluscs	
Roscanvel	SRQ3-KS39 (Poz-76862)	35	-11.5	2250 ± 30	1425 - 1292 (1359)	252 - 658 (A.D.)	Molluscs	Gregoire et al. (2017)
Roscanvel	SRQ3-KS39 (Beta-468468)	55-56	-11.5	2010 ± 30	1718 - 1514 (1616)	232 - 436 (A.D.)	Molluscs	
Roscanvel	SRQ3-KS39 (Poz-76863)	73	-11.5	2250 ± 30	1996 - 1716 (1856)	46 (B.C.) - 234 (A.D.)	Molluscs	Gregoire et al. (2017)
Roscanvel	SRQ3-KS39 (Poz-76864)	87-88	-11.5	2395 ± 30	2154 - 1896 (2025)	204 (B.C.) - 54 (A.D.)	Molluscs	Gregoire et al. (2017)
Roscanvel	SRQ3-KS39 (Poz-76837)	97	-11.5	2590 ± 30	2357 - 2143 (2250)	407 - 193 (B.C.)	Molluscs	Gregoire et al. (2017)
Roscanvel	SRQ3-KS39 (Poz-76838)	121	-11.5	4810 ± 30	5311 - 4959 (5135)	3361 - 3009 (B.C.)	Molluscs	Gregoire et al. (2017)
Roscanvel	SRQ3-KS39 (Poz-76840)	130	-11.5	7410 ± 40	8016 - 7788 (7902)	6066 - 5838 (B.C.)	Molluscs	Gregoire et al. (2017)
Roscanvel	SRQ3-KS40 (Beta-462612)	88-90	-19.6	1830 ± 30	1522 - 1308 (1415)	425 - 642 (A.D.)	Molluscs	
Fret	SRQ1-IS04 (Poz-68933)	41-42	-7.1	3320 ± 30	3277 - 3004 (3141)	1327 - 1054 (B.C.)	Benthic foram.	
Fret	SRQ1-IS04 (Poz-68934)	75-76	-7.1	3445 ± 35	3453 - 3206 (3330)	1503 - 1256 (B.C.)	Benthic foram.	
Fret	SRQ3-KS38 (Poz-76850)	26	-13.7	1635 ± 30	1312 - 1171 (1242)	638 - 779 (A.D.)	Molluscs	
Fret	SRQ3-KS38 (Poz-76851)	89	-13.7	2105 ± 35	1826 - 1560 (1693)	124 - 390 (A.D.)	Molluscs	
Fret	SRQ3-KS38 (Poz-85263)	101-103	-13.7	2030 ± 30	1740 - 1519 (1630)	210 - 431 (A.D.)	Maerl	
Fret	SRQ3-KS38 (Poz-76852)	115	-13.7	4700 ± 40	5071 - 4840 (4956)	3121 - 2890 (B.C.)	Molluscs	
Fret	SRQ3-KS38 (Poz-76853)	210	-13.7	4605 ± 35	4979 - 4797 (4888)	3029 - 2847 (B.C.)	Molluscs	
Fret	SRQ3-KS38 (Poz-76855)	232	-13.7	7220 ± 40	7855 - 7613 (7734)	5905 - 5663 (B.C.)	Molluscs	
Fret	SRQ3-KS38 (Poz-76856)	304	-13.7	7330 ± 50	7954 - 7695 (7825)	6004 - 5741 (B.C.)	Molluscs	
Fret	SRQ3-KS38 (Poz-76857)	320	-13.7	7360 ± 50	7973 - 7707 (7840)	6023 - 5757 (B.C.)	Molluscs	
Lanveoc-Poulmic	SRQ1-IS23 (Beta-397594)	38	-4.0	450 ± 30	152 - 4 (78)	1798 - 1946 (A.D.)	Maerl	
Lanveoc-Poulmic	SRQ1-IS23 (Poz-65762)	63	-4.0	720 ± 30	519 - 417 (468)	1431 - 1103 (A.D.)	Maerl	
Lanveoc-Poulmic	SRQ1-IS28 (Poz-85162)	10-11	-9.7	620 ± 30	498 - 280 (389)	1452 - 1170 (A.D.)	Maerl	
Lanveoc-Poulmic	SRQ1-IS28 (Poz-89695)	21-22	-9.7	550 ± 30	231 - 130 (181)	1719 - 1611 (A.D.)	Molluscs	
Lanveoc-Poulmic	SRQ1-IS28 (Poz-85163)	26-27	-9.7	690 ± 30	505 - 309 (407)	1135 - 1011 (A.D.)	Maerl	
Lanveoc-Poulmic	SRQ1-IS28 (Poz-89696)	35-36	-9.7	740 ± 30	533 - 421 (477)	417 - 152 (A.D.)	Molluscs	
Lanveoc-Poulmic	SRQ1-IS28 (Poz-85164)	45	-9.7	690 ± 30	505 - 309 (407)	1135 - 1011 (A.D.)	Maerl	
Lanveoc-Poulmic	SRQ1-IS28 (Poz-89697)	52-53	-9.7	615 ± 30	497 - 275 (386)	1453 - 1205 (A.D.)	Molluscs	
Lanveoc-Poulmic	SRQ1-IS28 (Poz-85167)	63	-9.7	665 ± 30	501 - 302 (402)	1449 - 1648 (A.D.)	Maerl	
Lanveoc-Poulmic	SRQ1-IS28 (Poz-89698)	66-67	-9.7	725 ± 30	522 - 418 (477)	1431 - 1532 (A.D.)	Molluscs	
Lanveoc-Poulmic	SRQ1-IS28 (Poz-85168)	70	34	740 ± 30	533 - 421 (477)	1417 - 1529 (A.D.)	Maerl	
Lanveoc-Poulmic	SRQ3-KS35 (Beta-462615)	82-84	-9.8	1980 ± 30	1638 - 1412 (1525)	312 - 538 (A.D.)	Molluscs	
Aulne	SRQ3-KS20 (Poz-76810)	35	-8.2	1925 ± 30	1612 - 1371 (1491)	338 - 579 (A.D.)	Molluscs	
Aulne	SRQ3-KS20 (Poz-76811)	92	-8.2	2380 ± 30	2151 - 1887 (2020)	701 (B.C.) - 62 (A.D.)	Molluscs	
Aulne	SRQ3-KS20 (Poz-76812)	114	-8.2	7070 ± 40	7600 - 7499 (7594)	5738 - 5549 (B.C.)	Molluscs	
Aulne	SRQ3-KS20 (Poz-76813)	140	-8.2	7480 ± 50	772 - 847 (7960)	6122 - 5897 (B.C.)	Molluscs	
Aulne	SRQ3-KS22 (Poz-78271)	2-3	25	1180 ± 30	87 - 676 (773)	1080 - 1274 (A.D.)	Molluscs	Lambert (2017)
Aulne	SRQ3-KS22 (SacA49421)	7	25	990 ± 30	616 - 480 (598)	1288 - 1417 (A.D.)	Molluscs	Lambert (2017)
Aulne	SRQ3-KS22 (SacA47758)	25	25	890 ± 30	616 - 480 (548)	1334 - 1470 (A.D.)	Molluscs	Lambert (2017)
Aulne	SRQ3-KS22 (SacA49422)	50	25	1180 ± 30	755 - 880 (968)	895 - 1070 (A.D.)	Molluscs	Lambert (2017)
Aulne	SRQ3-KS22 (Poz-78273)	94-95	25	1515 ± 30	1220 - 1005 (1113)	730 - 945 (A.D.)	Molluscs	Lambert (2017)
Aulne	SRQ3-KS22 (Poz-85262)	110-112	25	1425 ± 30	1099 - 928 (1014)	851 - 1022 (A.D.)	Maerl	
Daoulas	SRQ1-IS07 (Poz-68936)	65-67	-1.4	498 ± 30	498 - 280 (389)	1452 - 1670 (A.D.)	Molluscs	
Daoulas	SRQ1-IS21 (Poz-85169)	25-26	-8.4	560 ± 30	230 - 131 (181)	1720 - 1819 (A.D.)	Molluscs	
Daoulas	SRQ1-IS21 (Poz-85171)	34-35	-8.4	670 ± 30	501 - 304 (403)	1449 - 1646 (A.D.)	Maerl	
Daoulas	SRQ1-IS21 (Poz-85170)	45-46	-8.4	675 ± 30	502 - 306 (404)	1448 - 1644 (A.D.)	Maerl	
Daoulas	SRQ1-IS21 (Poz-85173)	57-58	-8.4	770 ± 30	552 - 423 (488)	1398 - 1527 (A.D.)	Maerl	
Auberl'ac'h	AL2013_IS08 (Poz-85175)	33-34	-3.2	545 ± 30	232 - 124 (178)	1718 - 1826 (A.D.)	Maerl	
Auberl'ac'h	AL2013_IS08 (Poz-85265)	45-46	-3.2	670 ± 30	501 - 304 (403)	1449 - 1646 (A.D.)	Maerl	
Auberl'ac'h	AL2013_IS08 (Poz-85255)	63-64	-3.2	650 ± 30	499 - 294 (397)	1451 - 1656 (A.D.)	Maerl	
Auberl'ac'h	ESCALICO-KS02 (Poz-85159)	0	-3.2	690 ± 30	456 - 289 (373)	1494 - 1661 (A.D.)	Molluscs	Lambert et al. (2020)
Auberl'ac'h	ESCALICO-KS02 (SacA49423)	0	-3.2	1430 ± 30	1125 - 924 (1025)	825 - 1026 (A.D.)	Molluscs	Lambert et al. (2020)
Auberl'ac'h	ESCALICO-KS02 (SacA47761)	0	-3.2	1740 ± 40	1438 - 1238 (1338)	512 - 712 (A.D.)	Molluscs	Lambert et al. (2020)
Auberl'ac'h	ESCALICO-KS02 (Poz-78153)	85-86	-3.2	1850 ± 30	1530 - 1338 (1434)	420 - 612 (A.D.)	Molluscs	Lambert et al. (2020)
Auberl'ac'h	ESCALICO-KS02 (SacA45622)	180-181	-3.2	2040 ± 30	1769 - 1546 (1658)	181 - 404 (A.D.)	Molluscs	Lambert et al. (2020)
Auberl'ac'h	ESCALICO-KS02 (Poz-78154)	180-181	-3.2	2075 ± 35	1814 - 1575 (1695)	136 - 375 (A.D.)	Molluscs	Lambert et al. (2020)
Auberl'ac'h	ESCALICO-KS02 (SacA45633)	180-181	-3.2	2515 ± 30	2320 - 2124 (2222)	370 - 174 (B.C.)	Molluscs	Lambert et al. (2020)
Auberl'ac'h	SRQ3-KS34 (Poz-76861)	20	-10.0	990 ± 30	686 - 546 (616)	1264 - 1404 (A.D.)	Molluscs	Gregoire et al. (2017)
Auberl'ac'h	SRQ3-KS34 (Poz-76862)	29-30	-10.0	980 ± 30	681 - 544 (613)	1269 - 1406 (A.D.)	Molluscs	
Auberl'ac'h	SRQ3-KS34 (Poz-9470)	42-43	-10.0	1475 ± 30	1183 - 953 (1068)	767 - 997 (A.D.)	Molluscs	
Auberl'ac'h	SRQ3-KS34 (Poz-9471)	61-62	-10.0	1575 ± 30	1288 - 1060 (1174)	662 - 890 (A.D.)	Molluscs	
Auberl'ac'h	SRQ3-KS34 (Poz-76863)	71-72	-10.0	1605 ± 30	1296 - 1168 (1232)	654 - 782 (A.D.)	Molluscs	
Auberl'ac'h	SRQ3-KS34 (Poz-76816)	80	-10.0	1670 ± 30	1368 - 1175 (1272)	582 - 775 (A.D.)	Molluscs	Gregoire et al. (2017)
Auberl'ac'h	SRQ3-KS34 (Beta-462613)	110-112	-10.0	1840 ± 30	1525 - 1311 (1418)	425 - 639 (A.D.)	Molluscs	
Auberl'ac'h	SRQ3-KS34 (Beta-462614)	130-132	-10.0	1980 ± 30	1637 - 1412 (1525)	313 - 538 (A.D.)	Molluscs	
Auberl'ac'h	SRQ3-KS34 (Poz-76817)	163	-10.0	2200 ± 30	1935 - 1695 (1815)	15 - 255 (A.D.)	Molluscs	Gregoire et al. (2017)
Auberl'ac'h	SRQ3-KS34 (Poz-85261)	171-172	-10.0	2170 ± 30	1896 - 1687 (1792)	54 - 263 (A.D.)	Maerl	
Auberl'ac'h	SRQ3-KS34 (Poz-76818)	181	-10.0	3035 ± 30	2927 - 2747 (2837)	977 - 797 (B.C.)	Molluscs	
Auberl'ac'h	SRQ3-KS34 (Poz-76820)	220	-10.0	3325 ± 30	3347 - 3020 (3184)	1397 - 1070 (B.C.)	Molluscs	Gregoire et al. (2017)
Auberl'ac'h	SRQ3-KS34 (Poz-76821)	260	-10.0	5590 ± 40	6195 - 5914 (6055)	4245 - 3964 (B.C.)	Molluscs	Gregoire et al. (2017)
Auberl'ac'h	SRQ3-KS36 (Beta-468469)	23-24	-13.1	880 ± 30	653 - 576 (615)	1297 - 1374 (A.D.)	Molluscs	
Auberl'ac'h	SRQ3-KS36 (Poz-76823)	40	-13.1	1520 ± 40	1264 - 980 (1122)	686 - 970 (A.D.)	Molluscs	
Auberl'ac'h	SRQ3-KS36 (Poz-76824)	145	-13.1	2350 ± 30	2128 - 1871 (2000)	178 (B.C.) - 79 (A.D.)	Molluscs	
Auberl'ac'h	SRQ3-KS36 (Poz-76825)	164	-13.1	2245 ± 30	1955 - 1727 (1841)	5 (B.C.) - 223 (A.D.)	Molluscs	
Brest - Elorn	SRQ1-IS17 (Beta-397593)	29	-2.0	1330 ± 30	1006 - 789 (898)	944 - 1161 (A.D.)	Maerl	
Brest - Elorn	SRQ1-IS17 (Poz-65761)	58	-2.0	1405 ± 30	1099 - 916 (1008)	851 - 1034 (A.D.)	Maerl	
Brest - Elorn	SRQ1-IS32 (Poz-85256)	12-13	-2.5	1385 ± 30	1087 - 901 (994)	863 - 1049 (A.D.)	Maerl	
Brest - Elorn	SRQ1-IS32 (Poz-89699)	22-23	-2.5	1400 ± 30	1149 - 911 (1030)	801 - 1039 (A.D.)	Molluscs	
Brest - Elorn	SRQ1-IS32 (Poz-85257)	27-29	-2.5	1470 ± 30	1182 - 937 (1060)	768 - 1013 (A.D.)	Maerl	
Brest - Elorn	SRQ1-IS32 (Poz-89692)	34-35	-2.5	1470 ± 30	1182 - 937 (1060)	768 - 1013 (A.D.)	Molluscs	
Brest - Elorn	SRQ1-IS32 (Poz-85258)	40-41	-2.5	1410 ± 30	1097 - 920 (1009)	853 - 1030 (A.D.)	Maerl	
Brest - Elorn	SRQ1-IS32 (Poz-89693)	45-46	-2.5	1480 ± 30	1184 - 954 (1069)	766 - 996 (A.D.)	Molluscs	
Brest - Elorn	SRQ1-IS32 (Poz-85259)	53-54	-2.5	1410 ± 30	1097 - 920 (1009)	853 - 1030 (A.D.)	Maerl	
Brest - Elorn	SRQ1-IS32 (Poz-89694)	60-61	-2.5	1435 ± 30	1150 - 931 (1041)	800 - 1019 (A.D.)	Molluscs	
Brest - Elorn	SRQ1-IS32 (Poz-85260)	64-65	-2.5	1465 ± 30	1181 - 935 (1058)	769 - 1015 (A.D.)	Maerl	
Brest - Elorn	SRQ3-KS44 (Poz-76826)	35	-6.2	2275 ± 30	2004 - 1736 (1870)	54 (B.C.) - 214 (A.D.)	Molluscs	
Brest - Elorn	SRQ3-VZ33 (Poz-122703)	65	-9.8	1730 ± 30	1408 - 1255 (1332)	542 - 695 (A.D.)	Molluscs	
Brest - Elorn	SRQ3-KS04 (Poz-122702)	149	-7	2290 ± 30	2060 - 1806 (1933)	110 (B.C.) - 144 (A.D.)	Molluscs	
Brest - Elorn	PAL-KS05 (Poz-102087)	40-42	-3.1	1360 ± 30	1063 - 892 (978)	887 - 1058 (A.D.)	Molluscs	
Brest - Elorn	PAL-KS05 (Poz-102088)	53-53	-3.1	1380 ± 30	1082 - 898 (990)	868 - 1052 (A.D.)	Molluscs	
Brest - Elorn	PAL-KS05 (Poz-102089)	69-71	-3.1	1425 ± 30	1099 - 928 (1014)	851 - 1022 (A.D.)	Molluscs	
Brest - Elorn	PAL-KS05 (Poz-102090)	88-90	-3.1	1475 ± 30	1183 - 953 (1068)	767 - 997 (A.D.)	Molluscs	
Brest - Elorn	PAL-KS05 (Poz-102091)	112-114	-3.1	1530 ± 30	1269 - 1047 (1158)	681 - 903 (A.D.)	Molluscs	
Brest - Elorn	PAL-KS05 (Poz-102092)	143.5-145.5	-3.1	1685 ± 30	1366 - 1180 (1273)	584 - 770 (A.D.)	Molluscs	
Brest - Elorn	PAL-KS05 (Poz-102093)	176-178	-3.1	1845 ± 30	1528 - 1313 (1421)	422 - 637 (A.D.)	Molluscs	
Brest - Elorn	PAL-KS05 (Poz-102159)	200-202	-3.1	1835 ± 30	1525 - 1310 (1418)	425 - 640 (A.D.)	Molluscs	
Brest - Elorn	PAL-KS05 (Poz-102160)	220-221	-3.1	2515 ± 35	2338 - 2046 (2192)	388 - 96 (B.C.)	Molluscs	
Brest - Elorn	PAL-KS05 (Poz-102161)	255-258	-3.1	3185 ± 35	3163 - 2847 (3005)	1213 - 897 (B.C.)	Molluscs	

Table 1: Table summarizing ^{14}C radiocarbon dating used for this study

(correction according to age reservoir and calibration).

Subregions of Brest Bay	Core name	Levels (name) in Figs. 8-11	Level bsf (cm) in Fig. 8-11	Maerl bed thickness (cm)	Sedimentation rate (mm/yr) (Fig. 16)	Level age (yr) based on sedimentation rate (LASR)	Accumulation rate (cm/yr - m/kyr)	Theoretical level age (yr) based on annual growing rate (0,25mm/yr) (TLA)	TLA/LASR	Maerl species
Lanveoc Poulmic cove	SRQ1-IS28	MB4	10 - 19	9,00	1,5	60	0,15 - 1,5	360	6,00	<i>Lithothamnion corallioides</i>
Lanveoc Poulmic cove	SRQ1-IS28	MB3	40 - 46	6,00	1,50	30	0,2 - 2	240	8,00	<i>Lithothamnion corallioides</i>
Lanveoc Poulmic cove	SRQ1-IS28	MB2	60 - 64,5	4,5	1,67	34	0,13 - 1,3	180	5,29	<i>Lithothamnion corallioides</i>
Lanveoc Poulmic cove	SRQ1-IS28	MB1	67 - 70	3,00	1,67	21	0,14 - 1,4	120	5,71	<i>Lithothamnion corallioides</i>
Auberlac'h cove	SRQ3-KS34	MB11	45 - 53,5	8,5	1,79	47	0,16 - 1,6	340	7,23	<i>Lithothamnion corallioides</i>
Auberlac'h cove	SRQ3-KS34	MB10	56,1 - 61,3	5,2	1,79	29	0,19 - 1,9	208	7,17	<i>Lithothamnion corallioides</i>
Auberlac'h cove	SRQ3-KS34	MB9	67 - 69	2,00	1,89	11	0,22 - 2,2	80	7,27	<i>Lithothamnion corallioides</i>
Auberlac'h cove	SRQ3-KS34	MB8	90 - 98,5	8,5	2,12	40	0,22 - 2,2	340	8,50	<i>Lithothamnion corallioides</i>
Auberlac'h cove	SRQ3-KS34	MB7	103 - 108,8	5,8	2,12	27	0,22 - 2,2	232	8,59	<i>Lithothamnion corallioides</i>
Auberlac'h cove	SRQ3-KS34	MB6	110 - 119,5	9,5	1,87	51	0,19 - 1,9	380	7,45	<i>Lithothamnion corallioides</i>
Auberlac'h cove	SRQ3-KS34	MB5	123,3 - 125	1,7	1,87	9	0,17 - 1,7	68	7,56	<i>Lithothamnion corallioides</i>
Auberlac'h cove	SRQ3-KS34	MB4	130 - 134,8	4,8	1,14	42	0,15 - 1,5	192	4,57	<i>Lithothamnion corallioides</i>
Auberlac'h cove	SRQ3-KS34	MB3	137,8 - 144,5	6,7	1,14	59	0,16 - 1,6	268	4,54	<i>Lithothamnion corallioides</i>
Auberlac'h cove	SRQ3-KS34	MB2	145,9 - 151,8	5,9	1,14	52	0,11 - 1,1	236	4,54	<i>Lithothamnion corallioides</i>

Table 2: Accumulation rates of rhodolith beds calculated for two cores in the Bay of Brest (SRQ1-IS28 and SRQ3-KS34). The age of each maerl bed was extrapolated from a local age-depth model.

Sites in the Bay of Brest	Sample and lab. no.	Core depth (cm)	Altitude LLTL (m)	AMS ¹⁴ C ages (radiocarbon yr B.P.)	Calibrated aged cal yr B.P. (mean) (2σ) ΔR = 46	Age cal (A)
Roscanvel	SRQ1-IS03 (Beta-397592)	24	-1.8	1260 ± 30	937 - 732 (835)	1013 - 12
Roscanvel	SRQ1-IS03 (Poz-65763)	46-47	-1.8	4175 ± 35	4420 - 4141 (4282)	2471 - 2
Roscanvel	SRQ3-KS39 (Poz-76861)	8	-11.5	740 ± 30	533 - 421 (477)	1417 - 15
Roscanvel	SRQ3-KS39 (Beta-468466)	15-16	-11.5	880 ± 30	653 - 576 (615)	1297 - 13
Roscanvel	SRQ3-KS39 (Beta-468467)	25-26	-11.5	1690 ± 30	1378 - 1217 (1298)	572 - 7
Roscanvel	SRQ3-KS39 (Poz-76862)	35	-11.5	1800 ± 40	1425 - 1292 (1359)	252 - 6
Roscanvel	SRQ3-KS39 (Beta-468468)	55-56	-11.5	2010 ± 30	1718 - 1514 (1616)	232 - 4
Roscanvel	SRQ3-KS39 (Poz-76863)	73	-11.5	2250 ± 30	1996 - 1716 (1856)	46 (B.C.) -
Roscanvel	SRQ3-KS39 (Poz-76864)	87-88	-11.5	2395 ± 30	2154 - 1896 (2025)	204 (B.C.) -
Roscanvel	SRQ3-KS39 (Poz-76837)	97	-11.5	2590 ± 30	2357 - 2143 (2250)	407 - 1
Roscanvel	SRQ3-KS39 (Poz-76838)	121	-11.5	4810 ± 30	5311 - 4959 (5135)	3361 - 30
Roscanvel	SRQ3-KS39 (Poz-76840)	130	-11.5	7410 ± 40	8016 - 7788 (7902)	6066 - 58
Roscanvel	SRQ3-KS40 (Beta-462612)	88-90	-19.6	1830 ± 30	1522 - 1308 (1415)	425 - 6
Fret	SRQ1-IS04 (Poz-68933)	41-42	-7.1	3320 ± 30	3277 - 3004 (3141)	1327 - 10
Fret	SRQ1-IS04 (Poz-68934)	75-76	-7.1	3445 ± 35	3453 - 3206 (3330)	1503 - 12
Fret	SRQ3-KS38 (Poz-76850)	26	-13.7	1635 ± 30	1312 - 1171 (1242)	638 - 7
Fret	SRQ3-KS38 (Poz-76851)	89	-13.7	2105 ± 35	1826 - 1560 (1693)	124 - 3
Fret	SRQ3-KS38 (Poz-85263)	101-103	-13.7	2030 ± 30	1740 - 1519 (1630)	210 - 4
Fret	SRQ3-KS38 (Poz-76852)	115	-13.7	4700 ± 40	5071 - 4840 (4956)	3121 - 28
Fret	SRQ3-KS38 (Poz-76853)	110	-13.7	4605 ± 35	4979 - 4797 (4888)	3029 - 28
Fret	SRQ3-KS38 (Poz-76855)	232	-13.7	7220 ± 40	7855 - 7613 (7734)	5905 - 50
Fret	SRQ3-KS38 (Poz-76856)	304	-13.7	7330 ± 50	7954 - 7695 (7825)	6004 - 53
Fret	SRQ3-KS38 (Poz-76857)	320	-13.7	7360 ± 50	7973 - 7707 (7840)	6023 - 53
Lanveoc-Poulmic	SRQ1-IS23 (Beta-397594)	38	-4.0	450 ± 30	152 - 4 (78)	1798 - 19
Lanveoc-Poulmic	SRQ1-IS23 (Poz-65762)	63	-4.0	720 ± 30	519 - 417 (468)	1431 - 15
Lanveoc-Poulmic	SRQ1-IS28 (Poz-85162)	10-11	-9.7	620 ± 30	498 - 280 (389)	1452 - 16
Lanveoc-Poulmic	SRQ1-IS28 (Poz-85165)	21-22	-9.7	550 ± 30	231 - 130 (181)	1719 - 18
Lanveoc-Poulmic	SRQ1-IS28 (Poz-85163)	26-27	-9.7	690 ± 30	505 - 309 (407)	1445 - 16
Lanveoc-Poulmic	SRQ1-IS28 (Poz-85169)	35-36	-9.7	740 ± 30	533 - 421 (477)	1417 - 15
Lanveoc-Poulmic	SRQ1-IS23 (Poz-85164)	45	-9.7	690 ± 30	505 - 309 (407)	1445 - 16
Lanveoc-Poulmic	SRQ1-IS28 (Poz-89697)	52-53	-9.7	615 ± 30	497 - 275 (386)	1453 - 16
Lanveoc-Poulmic	SRQ1-IS28 (Poz-85167)	63	-9.7	665 ± 30	501 - 302 (402)	1449 - 16
Lanveoc-Poulmic	SRQ1-IS28 (Poz-89698)	66-67	-9.7	725 ± 30	522 - 418 (470)	1428 - 15
Lanveoc-Poulmic	SRQ1-IS28 (Poz-85168)	70	34	740 ± 30	533 - 421 (477)	1417 - 15
Lanveoc-Poulmic	SRQ3-KS35 (Beta-462615)	82-84	-9.8	1980 ± 30	1638 - 1412 (1525)	312 - 5
Aulne	SRQ3-KS20 (Poz-76810)	35	-8.2	1925 ± 30	1612 - 1371 (1492)	338 - 5
Aulne	SRQ3-KS20 (Poz-76811)	92	-8.2	2380 ± 30	2151 - 1888 (2020)	201 (B.C.) -
Aulne	SRQ3-KS20 (Poz-76812)	114	-8.2	7070 ± 40	7688 - 7499 (7594)	5738 - 5
Aulne	SRQ3-KS20 (Poz-76813)	140	-8.2	7480 ± 50	8072 - 7847 (7960)	6122 - 58
Aulne	SRQ3-KS22 (Poz-78271)	2-3	25	1180 ± 30	870 - 676 (773)	1080 - 12
Aulne	SRQ3-KS22 (SacA49421)	7	25	990 ± 30	662 - 533 (598)	1288 - 14
Aulne	SRQ3-KS22 (SacA47758)	25	25	890 ± 30	616 - 480 (548)	1334 - 14
Aulne	SRQ3-KS22 (SacA49422)	50	25	1370 ± 30	1055 - 880 (968)	895 - 10
Aulne	SRQ3-KS22 (Poz-78273)	94-95	25	1515 ± 30	1220 - 1005 (1113)	730 - 9
Aulne	SRQ3-KS22 (Poz-85262)	110-112	25	1425 ± 30	1099 - 928 (1014)	851 - 10
Daoulas	SRQ1-IS07 (Poz-68936)	65-67	-1.4	620 ± 30	498 - 280 (389)	1452 - 16
Daoulas	SRQ1-IS21 (Poz-85169)	25-26	-8.4	560 ± 40	230 - 131 (181)	1720 - 18
Daoulas	SRQ1-IS21 (Poz-85171)	34-35	-8.4	670 ± 30	501 - 304 (403)	1449 - 16

Daoulas	SRQ1-IS21 (Poz-85170)	45-46	-8.4	675 ± 30	502 - 306 (404)	1448 - 16
Daoulas	SRQ1-IS21 (Poz-85173)	57-58	-8.4	770 ± 30	552 - 423 (488)	1398 - 15
Auberlac'h	AL2013_IS08 (Poz-85175)	33-34	-3.9	545 ± 30	232 - 124 (178)	1718 - 18
Auberlac'h	AL2013_IS08 (Poz-85265)	45-46	-3.9	670 ± 30	501 - 304 (403)	1449 - 16
Auberlac'h	AL2013_IS08 (Poz-85255)	63-64	-3.9	650 ± 30	499 - 294 (397)	1451 - 16
Auberlac'h	ESCALICO-KS02 (Poz-85159)	2	-3.2	690 ± 30	456 - 289 (373)	1494 - 16
Auberlac'h	ESCALICO-KS02 (SacA49423)	20	-3.2	1430 ± 30	1125 - 924 (1025)	825 - 10
Auberlac'h	ESCALICO-KS02 (SacA47761)	42	-3.2	1740 ± 40	1438 - 1238 (1338)	512 - 7
Auberlac'h	ESCALICO-KS02 (Poz-78153)	85-86	-3.2	1850 ± 30	1530 - 1338 (1434)	420 - 6
Auberlac'h	ESCALICO-KS02 (SacA45632)	140-141	-3.2	2040 ± 30	1769 - 1546 (1658)	181 - 4
Auberlac'h	ESCALICO-KS02 (Poz-78154)	180-181	-3.2	2075 ± 35	1814 - 1575 (1695)	136 - 3
Auberlac'h	ESCALICO-KS02 (SacA45633)	249-250	-3.2	2515 ± 30	2320 - 2124 (2222)	370 - 1
Auberlac'h	SRQ3-KS34 (Poz-76814)	20	-10.0	990 ± 30	686 - 546 (616)	1264 - 14
Auberlac'h	SRQ3-KS34 (Poz-94708)	29-30	-10.0	980 ± 30	681 - 544 (613)	1269 - 14
Auberlac'h	SRQ3-KS34 (Poz-94709)	42-43	-10.0	1475 ± 30	1183 - 953 (1068)	767 - 99
Auberlac'h	SRQ3-KS34 (Poz-94710)	61-62	-10.0	1775 ± 30	1288 - 1060 (1174)	662 - 8
Auberlac'h	SRQ3-KS34 (Poz-94711)	71-72	-10.0	1605 ± 30	1296 - 1168 (1232)	654 - 7
Auberlac'h	SRQ3-KS34 (Poz-76816)	80	-10.0	1670 ± 30	1368 - 1175 (1272)	582 - 7
Auberlac'h	SRQ3-KS34 (Beta-462613)	110-112	-10.0	1840 ± 30	1525 - 1311 (1418)	425 - 6
Auberlac'h	SRQ3-KS34 (Beta-462614)	130-132	-10.0	1980 ± 30	1637 - 1412 (1525)	313 - 5
Auberlac'h	SRQ3-KS34 (Poz-76817)	163	-10.0	2200 ± 30	1935 - 1695 (1815)	15 - 25
Auberlac'h	SRQ3-KS34 (Poz-85261)	171-172	-10.0	2170 ± 30	1896 - 1687 (1792)	54 - 26
Auberlac'h	SRQ3-KS34 (Poz-76818)	181	-10.0	3035 ± 30	2927 - 2747 (2837)	977 - 7
Auberlac'h	SRQ3-KS34 (Poz-76820)	20	-10.0	3325 ± 30	3347 - 3020 (3184)	1397 - 10
Auberlac'h	SRQ3-KS34 (Poz-76821)	26	-10.0	5590 ± 40	6195 - 5914 (6055)	4245 - 35
Auberlac'h	SRQ3-KS36 (Beta-468469)	23-24	-13.1	880 ± 30	653 - 576 (615)	1297 - 13
Auberlac'h	SRQ3-KS36 (Poz-76823)	40	-13.1	1520 ± 40	1264 - 980 (1122)	686 - 9
Auberlac'h	SRQ3-KS36 (Poz-76824)	145	-13.1	2350 ± 30	2128 - 1871 (2000)	178 (B.C.) -
Auberlac'h	SRQ3-KS36 (Poz-76825)	164	-13.1	2245 ± 30	1955 - 1727 (1841)	5 (B.C.) -
Brest - Elorn	SRQ1-IS17 (Beta-394595)	29	-2.0	1330 ± 30	1006 - 789 (898)	944 - 11
Brest - Elorn	SRQ1-IS17 (Poz-85761)	58	-2.0	1405 ± 30	1099 - 916 (1008)	851 - 10
Brest - Elorn	SRQ1-IS32 (Poz-85256)	12-13	-2.5	1385 ± 30	1087 - 901 (994)	863 - 10
Brest - Elorn	SRQ1-IS32 (Poz-85699)	22-23	-2.5	1400 ± 30	1149 - 911 (1030)	801 - 10
Brest - Elorn	SRQ1-IS32 (Poz-85257)	27-29	-2.5	1470 ± 30	1182 - 937 (1060)	768 - 10
Brest - Elorn	SRQ1-IS32 (Poz-89692)	34-35	-2.5	1470 ± 30	1182 - 937 (1060)	768 - 10
Brest - Elorn	SRQ1-IS32 (Poz-85258)	40-41	-2.5	1410 ± 30	1097 - 920 (1009)	853 - 10
Brest - Elorn	SRQ1-IS32 (Poz-89693)	45-46	-2.5	1480 ± 30	1184 - 954 (1069)	766 - 9
Brest - Elorn	SRQ1-IS32 (Poz-85259)	53-54	-2.5	1410 ± 30	1097 - 920 (1009)	853 - 10
Brest - Elorn	SRQ1-IS32 (Poz-89694)	60-61	-2.5	1435 ± 30	1150 - 931 (1041)	800 - 10
Brest - Elorn	SRQ1-IS32 (Poz-85260)	64-65	-2.5	1465 ± 30	1181 - 935 (1058)	769 - 10
Brest - Elorn	SRQ3-KS44 (Poz-76826)	35	-6.2	2275 ± 30	2004 - 1736 (1870)	54 (B.C.) -
Brest - Elorn	SRQ3-VZ33 (Poz-122703)	65	-9.8	1730 ± 30	1408 - 1255 (1332)	542 - 6
Brest - Elorn	SRQ3-KS04 (Poz-122702)	149	-7	2290 ± 30	2060 - 1806 (1933)	110 (B.C.) -
Brest - Elorn	PAL-KS05 (Poz-102087)	40-42	-3.1	1360 ± 30	1063 - 892 (978)	887 - 10
Brest - Elorn	PAL-KS05 (Poz-102088)	53-53	-3.1	1380 ± 30	1082 - 898 (990)	868 - 10
Brest - Elorn	PAL-KS05 (Poz-102089)	69-71	-3.1	1425 ± 30	1099 - 928 (1014)	851 - 10
Brest - Elorn	PAL-KS05 (Poz-102090)	88-90	-3.1	1475 ± 30	1183 - 953 (1068)	767 - 9
Brest - Elorn	PAL-KS05 (Poz-102091)	112-114	-3.1	1530 ± 30	1269 - 1047 (1158)	681 - 9
Brest - Elorn	PAL-KS05 (Poz-102092)	143,5-145,5	-3.1	1685 ± 30	1366 - 1180 (1273)	584 - 7
Brest - Elorn	PAL-KS05 (Poz-102093)	176-178	-3.1	1845 ± 30	1528 - 1313 (1421)	422 - 6
Brest - Elorn	PAL-KS05 (Poz-102159)	200-202	-3.1	1835 ± 30	1525 - 1310 (1418)	425 - 6
Brest - Elorn	PAL-KS05 (Poz-102160)	220-221	-3.1	2515 ± 35	2338 - 2046 (2192)	388 - 9

Journal Pre-proof

Subregions of the Bay of Brest	Core name	Levels (name) in figs. 8-11	Level bsf (cm) in fig. 8-11	Maerl bed thickness (cm)	Sedimentation rate (mm/yr) (fig. 16)	Level age (yr) based on sedimentation rate (LASR)	Accumulation rate (cm/yr - m/kyr)	Theoretical (yr) based on growing rate (mm/yr)
Lanveoc Poulmic cove	SRQ1-IS28	MBF4	10 - 19	9,00	1,5	60	0,15 - 1,5	36
Lanveoc Poulmic cove	SRQ1-IS28	MBF3	40 - 46	6,00	1,50	30	0,2 - 2	24
Lanveoc Poulmic cove	SRQ1-IS28	MBF2	60 - 64,5	4,5	1,67	34	0,13 - 1,3	18
Lanveoc Poulmic cove	SRQ1-IS28	MBF1	67 - 70	3,00	1,67	21	0,14 - 1,4	12
Auberlac'h cove	SRQ3-KS34	MBF11	45 - 53,5	8,5	1,79	47	0,16 - 1,6	34
Auberlac'h cove	SRQ3-KS34	MBF10	56,1 - 61,3	5,2	1,79	29	0,19 - 1,9	20
Auberlac'h cove	SRQ3-KS34	MBF9	67 - 69	2,00	1,89	11	0,22 - 2,2	80
Auberlac'h cove	SRQ3-KS34	MBF8	90 - 98,5	8,5	2,12	40	0,22 - 2,2	34
Auberlac'h cove	SRQ3-KS34	MBF7	103 - 108,8	5,8	2,12	27	0,22 - 2,2	23
Auberlac'h cove	SRQ3-KS34	MBF6	110 - 119,5	9,5	1,87	51	0,19 - 1,9	38
Auberlac'h cove	SRQ3-KS34	MBF5	123,3 - 125	1,7	1,87	9	0,17 - 1,7	68
Auberlac'h cove	SRQ3-KS34	MBF4	130 - 134,8	4,8	1,14	42	0,15 - 1,5	19
Auberlac'h cove	SRQ3-KS34	MBF3	137,8 - 144,5	6,7	1,14	59	0,16 - 1,6	26
Auberlac'h cove	SRQ3-KS34	MBF2	145,9 - 151,8	5,9	1,14	52	0,11 - 1,1	23

Highlights

- Stratigraphy of late-Holocene estuarine sediments reveals interbedded maerl beds
- First maerl occurrence in the Bay of Brest is dated around 2000 cal yr BP
- Development of maerl beds coincides with the onset of colder and drier climates
- Maerl building phases are disrupted by periods of climate deterioration
- Coarse sedimentary deposits are associated with increased paleostorm activity

Journal Pre-proof

Declaration of interests

☒ The authors declare that they have no known competing financial interests or personal relationships that could have appeared to influence the work reported in this paper.

☐ The authors declare the following financial interests/personal relationships which may be considered as potential competing interests:

Journal Pre-proof